Chem Soc Rev

Review ARTICLE

Preparation of Two Dimensional Layered Double Hydroxide Nanosheets and Their Applications

Jingfang Yu,[a, b, c] Qiang Wang,[d] Dermot O'Hare,[*c] Luyi Sun[*a, b]

Received 00th January 20xx,
Accepted 00th January 20xx

DOI: 10.1039/x0xx00000x

www.rsc.org/

Layered double hydroxides (LDHs) with their highly flexible and tunable chemical composition and physical properties have attracted tremendous attention in recent years. LDHs have found widespread application as catalysts, anion exchange materials, fire retardants, and nano-fillers in polymer nanocomposites. The ability to exfoliate LDHs into ultrathin nanosheets enables a range of new opportunities for multifunctional materials. In this review we summarize the current available LDHs exfoliation methods. In particular, we highlight recent developments for the direct synthesis of single-layer LDH nanosheets, as well as the emerging applications of LDH nanosheets in catalyzing oxygen evolution reactions and preparing light emitting devices, supercapacitors, and flame retardant nanocomposites.

1. Introduction

In recent years, inorganic layered materials at nanoscale have attracted intensive interest in the applications of novel nanocomposites,[1-15] ion exchangers,[16-20] photochemistry,[21-27] and catalysis.[28-41] Layered double hydroxides (LDHs), known as anionic clays, are one of the most thoroughly studied layered materials.[42-44] Positively charged metallic layers and interlayer anions and water comprise LDHs. The general formula of LDHs is $[M^{2+}_{1-x}M^{3+}_{x}(OH)_2]^{x+}[A^{p-}_{x/p}]^{x+}\bullet mH_2O$ (Figure 1), where M^{2+} and M^{3+} are metallic bivalent cation and metallic trivalent cation, respectively, and A^{n-} is interlayer anion. $X = M^{3+}/(M^{2+}+M^{3+})$ is surface charge determined by the ratio of the two metal cations, which is subject to change for various applications.

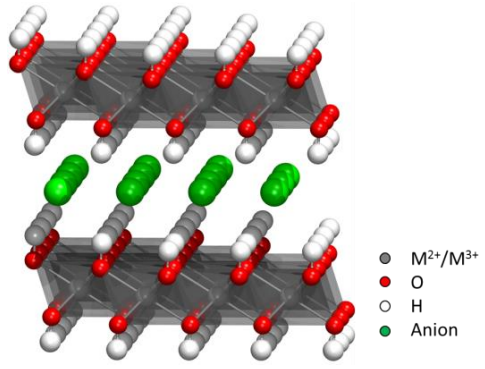

Figure 1. A typical structure of layered double hydroxide.[45] Reproduced with permission from reference 45. Copyright 2015 The Royal Society of Chemistry.

While LDHs have found widespread application (previous reviews on LDHs are discussed elsewhere[38, 42, 46-51]),[44, 52-55] in most cases their extent of application as well as overall performance are affected by the fact that the lamellar LDHs flakes tend to stack or even form bundles and agglomerations.[56] Exfoliating LDHs into single-layer nanosheets maximizes the utility of each single-layer, which possesses a high specific surface area.[57] Such single-layer nanosheets can be used for both fundamental studies and as a building block to fabricate a wide variety of functional nanostructured materials.[42, 58] A prevailing example is the layer-by-layer assembly of nanosheets with appropriately charged counterparts though a wet process.[58, 59] The preparation of LDH nanosheets has been extensively studied in the past two decades, and the exponentially growing applications of LDH nanosheets render it a research hotspot.[20, 60] There are typically two categories of approaches to synthesize LDH nanosheets: top-down exfoliation and bottom-up direct synthesis method. Exfoliation of layered materials often constitutes a two-step process: intercalating the layered materials first to increase the interlayer distance, followed by the exfoliation step to delaminate the layers. Bottom-up method typically refers to a one-step process that directly synthesizes inorganic nanosheets from appropriate precursors.

Synthesis of LDHs with a controllable size is the prerequisite to achieve nanosheets with different lateral dimensions and thus aspect ratio, as the thickness of any single-layer metal hydroxide nanosheet is fixed at ca. 0.48 nm.[42] Various methods have been developed to prepare LDHs with different sizes,[61-64] including co-precipitation of inorganic salts in basic solution at either low or high supersaturation, hydrothermal synthesis, re-construction, and ion-exchange methods.[42] To date, well defined large LDHs crystals (microns in diameter) can be prepared through the urea[65-67] (or hexamethylenetetramine[68]) hydrolysis method, which takes advantage of a phenomenon that urea is neutral at low temperatures but hydrolyzes above

[a] Department of Chemical & Biomolecular Engineering, University of Connecticut, Storrs, Connecticut 06269, United States. Email: luyi.sun@uconn.edu
[b] Polymer Program, Institute of Materials Science, University of Connecticut, Storrs, Connecticut 06269, United States.
[c] Chemistry Research Laboratory, Department of Chemistry, University of Oxford, 12 Mansfield Road, Oxford, OX1 3TA, UK. E-mail: dermot.ohare@chem.ox.ac.uk
[d] College of Environmental Science and Engineering, Beijing Forestry University, Beijing 100083, China.

90 °C to generate a basic solution. The homogenous and gradual increase of pH by urea hydrolysis facilitates the synthesis of LDHs with a high crystallinity and purity. On the other hand, co-precipitation methods (i.e., construction metal salts and base co-precipitating at supersaturated conditions) result in LDHs with a smaller size (tens to hundreds of nanometer in diameter), but it provides a time-saving process to synthesize LDHs with a relatively low crystallinity,[69, 70] which offers a relatively easy access to the interlayer region. There are two typical co-precipitation processes based on operation: (1) co-precipitation at high super-saturation, in which typically an M^{2+} and M^{3+} containing solution is added to a basic solution (a wider choices of metal cations are discussed in the review[42]) with desired interlayer containing anions and the reaction is stopped when reaching the set pH value; (2) co-precipitation at low super-saturation, in which two solutions, one containing construction metal cations and the other containing counter anions and precipitation base are mixed together drop by drop.

In this review article, methods to prepare LDH nanosheets are discussed in details based on different methodologies, with a focus on preparation mechanism. We also provide an overview of recent applications of LDH nanosheets, especially new applications in water splitting reaction, light emitting materials, polymer nanocomposites, and supercapacitors. The generalized formula for an LDH may be represented by $[M^{a+}_{x}M'^{b+}_{y}(OH)_2](^{ax+by-2)+}(A^{p-})_q$. Throughout the paper, we use M^{2+}_{n}/M^{3+}_{k}-A^{p-}-LDHs as the abbreviation for specific LDHs, where M^{2+} represents a divalent cation, M^{3+} represents a trivalent cation, the selection of metal cations is theoretically determined by the difference of their ionic radius[42]; *n* and *k* stands for the moles ratios of M^{2+} and M^{3+} correspondingly and they are usually omitted when the value is 1, and *A* stands for an interlayer anionic species.

2. Preparation of LDH nanosheets

Compared to other layered inorganic compounds, LDHs are difficult to be exfoliated due to their high layer charge density.[71] The exfoliation of LDHs was first observed when intercalating anionic organic guests (such as amino acids or surfactants) into the LDHs interlayer space and dispersed in certain solvents, usually with the assistance of ultrasonication (Figure 2). Later, exfoliation by an electrostatic repulsion in aqueous solution was developed.[72] More recently, exfoliation of LDHs without being pre-intercalated by organic species in interlayer galleries can be achieved by using formamide as the solvent, which is a more efficient way to achieve exfoliation. At present, more efficient approaches of preparing LDH nanosheets, such as laser ablation, take only several minutes to finish the exfoliation. Herein, we will discuss the developed exfoliation approaches of LDHs and the future of this area.

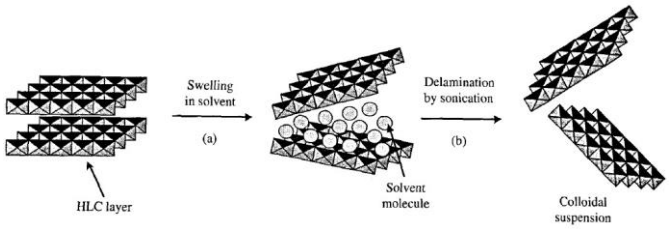

Figure 2. A general process to exfoliate LDHs.[73] Reproduced with permission from reference 73. Copyright 2010 American Scientific Publishers.

2.1 Tailoring interlayer environment for exfoliation

2.1.1 Exfoliation in alcohols

The very first attempt to exfoliate LDHs was achieved by Adachi-Pagano et al.[74] in 1999. The dodecyl sulfate (DS^-, $C_{12}H_{25}SO_4^-$) intercalated Zn_2/Al-DS^--LDHs was fully exfoliated in butanol dispersant. Zn_2/Al-DS^--LDHs could be completely exfoliated and remained stable for at least 8 months after refluxing in butanol at 120 °C for 16 hours. The concentration of the exfoliated Zn_2/Al-DS^--LDHs was reported as high as 1.5 g/L of butanol.[74] Higher alcohols such as pentanol and hexanol have also been proven successfully functioning as a dispersant. Other dispersants, such as water, methanol, ethanol, propanol, and hexane were examined under the same conditions as well. The results showed that Zn_2/Al-DS^--LDHs was only partially delaminated and dispersed in these solvents and the dispersions were unstable and settled down after a few hours. It was found that the hydration state of the DS^--LDHs is a vital factor towards complete exfoliation. Evidence shows that exfoliation was only achieved when the modified LDHs was previously dried under vacuum at room temperature for a day rather than a fresh wet prepared LDH was used, or the organo-modified LDHs was thoroughly dried under vacuum at 80 °C for a day. This vital LDHs hydration state towards exfoliation formed under intense drying. A new DS^- containing phase with a reduced interlayer distance of 1.68 nm formed with a single-layer of tilted and intertwined DS^- chains in the interlayer region. This new LDHs phase displayed a densely packed structure, rendering it less likely to be exfoliated. Thus, the possible exfoliation mechanism was proposed to be a rapid replacement of all of the intercalated water molecules by solvent molecules owing to the high boiling point of butanol under reflux conditions.

Slightly later, Singh et al.[75] studied the exfoliation of Li/Al_2-LDH intercalated with various surfactants following the exfoliation method developed by Adachi-Pagano et al.[74] Interestingly, the authors found that the intercalation of alkyl sulfate (sodium octyl sulfate (SOS) or sodium dodecyl sulfate (SDS)) did not lead to exfoliation whereas the intercalation of sodium 4-octylbenzenesulfonate (SOBS) and sodium dodecylbenzenesulfonate (SDBS) led to successful exfoliation. The underlying reason is that the exfoliation of this particular Li/Al_2-LDH depends on the alkyl chain length as well as the head group moiety of the intercalated surfactant.

In 2006, Venugopal et al.[76] expanded the exfoliation method to different kinds of divalent and trivalent metal bearing LDHs, including Mg/Al-, Ni/Al-, and Zn/Al-LDHs with either SDS or

SDBS as an intercalant in a wide range of dispersants including 1-butanol, 1-hexanol, 1-octanol, 1-decanol, n-hexane, and water. It turned out that the LDHs exfoliated better at low $[M^{2+}]/[M^{3+}]$ ratios and barely exfoliated in nonpolar solvents (e.g., hexane) while exfoliated best in alcohols, such as 1-butanol, 1-hexanol, 1-octanol, and 1-decanol. The degree of exfoliation and stability of the resultant colloids increased with an increasing size of the surfactant anion (DBS). However, delamination in water did not occur for any LDHs.[76]

2.1.2 Exfoliation in toluene

Due to the rising of polymer nanocomposites in recent decades, researchers are interested in exfoliating LDHs in non-polar solvents, so that the dispersed LDH nanosheets could be directly used to prepare various polymer nanocomposites. Jobbágy et al.[77] studied the exfoliation and restacking behavior of $Mg_{0.71}/Al_{0.29}$-DS^--LDH in CCl_4 or toluene in capped test tubes through a 30 min ultra-sonication with 2 h of equilibrium at room temperature. Figure 3 shows the XRD patterns of the translucent gels resulted from the hybrid dispersed in toluene (A) and CCl_4 (B). After being dispersed in toluene, DS^- intercalated LDH produced only a large expansion of the basal distance as shown in Figure 3. Whereas the one dispersed in CCl_4 showed complete loss of short range spatial arrangement, indicating a successful exfoliation. The conclusion was that delamination of LDHs intercalated with amphiphilic anions must be rationalized in terms of the miscibility of the intercalated LDHs and the selected solvent.

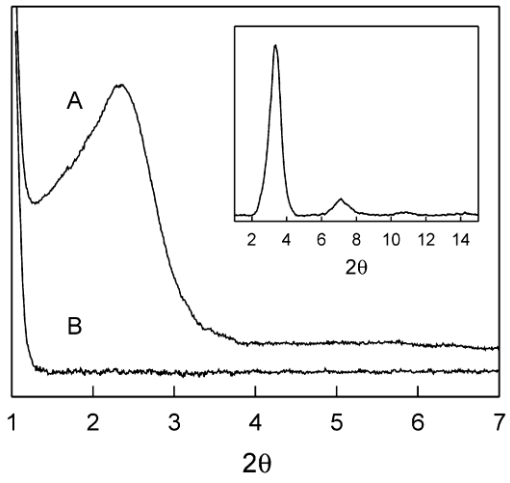

Figure 3. XRD patterns of (A) toluene-swollen and (B) CCl_4-delaminated LDHs-DS^- gels. The inset shows the *pattern* of the DS^- intercalated LDHs.[77] Reproduced with permission from reference 77. Copyright 2004 Elsevier Inc.

Toluene instead of butanol was studied as the dispersant of DS^- intercalated LDHs by Naik et al.[78] DS^- intercalated LDHs, including $Mg_{0.67}/Al_{0.33}$-LDHs and $Co_{0.67}/Al_{0.33}$-LDHs, can be dispersed in toluene. Rapid delamination occurred after stirring a pre-determined amount of DS^- intercalated LDHs in toluene followed by sonication for 5 min to obtain dispersions with different volume fractions. At lower volume fractions (≤0.005) of LDHs, a clear transparent dispersion was obtained which showed a clear Tyndall light scattering effect. It is worth noting that this process does not have a swelling state as the exfoliation process is too rapid and the gel state is the preferred state of the exfoliation dispersion (shown in Figure 4). The gel formation was proposed as a result of the attractive dispersive interactions of toluene molecules with the tails of the SDS chains anchored onto LDHs sheets.[79]

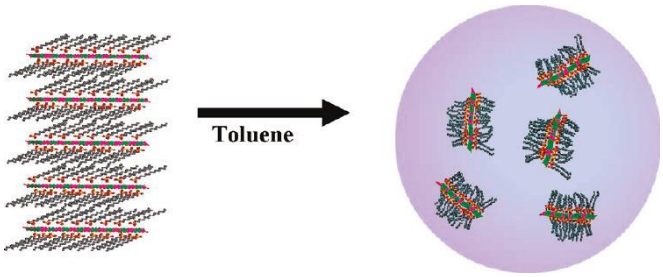

Figure 4. Schematic of the delamination of a surfactant-intercalated LDHs.[78] Reproduced with permission from reference 78. Copyright 2011 American Chemical Society.

The proposed mechanism of LDHs exfoliation was based on a recent molecular dynamics simulation showing that in layered compounds intercalated with long-chain surfactant molecules, dispersive or van der Waals interactions between the chains anchored onto opposing inorganic layers are responsible for holding the sheets together. Therefore, delamination was expected by disrupting or weakening the van der Waals interactions between the chains anchored on opposing layers. DS^- was used to convert the hydrophilic interlayer regime of LDHs into hydrophobic and to solvate the nonpolar solvent molecules (toluene).

2.1.3 Exfoliation in polymers/monomers

Other than intercalating LDHs with organic anions, researchers have directly intercalated polymers/monomers in between LDHs layers. For example, up to 10% of exfoliated LDHs can be dispersed into organic media as reported by O'Leary et al.[80] Various acrylate monomers, including 2-hydroxyethyl methacrylate (HEMA), ethyl methacrylate, methyl methacrylate, ethyl acrylate, and methyl acrylate, were investigated as the dispersant to exfoliate Mg_2/Al-DS^--LDH. A typical process is as follows: Mg_2/Al-DS^--LDH was added into an acrylate monomer at 70 °C, and the mixture was stirred at high shear for 20 min. After stopping heating and stirring, most of the solid remained in suspension after 24 hours of standing still. In 2-hydroxyethyl methacrylate, the exfoliated LDH nanosheets were stable for weeks. However, in the rest of the acrylate monomers, homogeneous suspensions formed, which separated into two parts after a couple of hours of standing still, i.e., pure monomers and a gelatinous suspension of LDHs.

The proposed mechanism is that the delamination can be promoted at high shear. The individual sheets of the layered materials were believed to be separated by being forced to slide over each other at a high shear. The X-ray diffraction (XRD) pattern showed an increase in d-spacing from 0.78 nm of Mg_2/Al-Cl^--LDH to 2.6 nm of Mg_2/Al-DS^--LDH (Figure 5a). A drop of a dilute exfoliated sample of Mg_2/Al-DS^--LDH in HEMA was dried under vacuum on a glass slide to form a thin white film. The XRD pattern of this film (Figure 5b) showed a very intensive

diffraction peak corresponding to a basal spacing of 2.6 nm and several much weaker diffractions. The intensity of the *001* Bragg reflection was ascribed to the preferential ordering of the layers parallel to the glass plate upon the evaporation of the monomers. However, the XRD pattern (Figure 5c) of the ground exfoliated LDH which was treated to polymerize the monomers followed by freeze drying with liquid nitrogen showed only a weak band attributed to the *001* Bragg reflection of Mg_2/Al-DS^--LDH exhibiting little long range order in the *c*-direction, indicating an almost complete exfoliation of LDH layers.

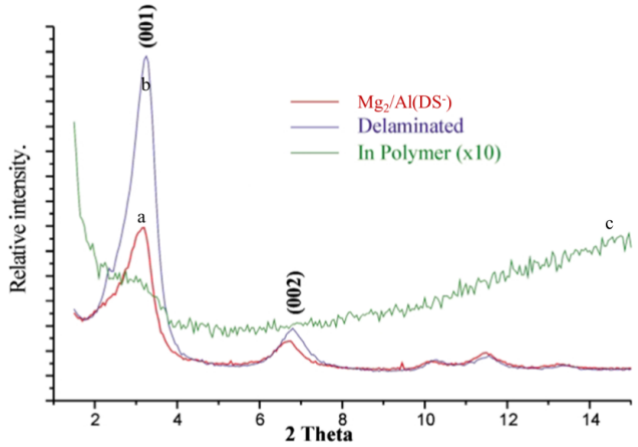

Figure 5. XRD patterns of (a) Mg_2/Al-DS^--LDH as prepared (red), (b) Mg_2/Al-DS^--LDH after delamination in HEMA and subsequent restacking (blue), and (c) Mg_2/Al-DS^--LDH (5 %) in polymerized HEMA (×10) (green). All patterns were obtained under identical conditions.[80] Reproduced with permission from reference 80. Copyright 2002 The Royal Society of Chemistry.

Zn_3/Al-LDH was reported to be fully exfoliated in polystyrene (PS) by Qiu et al.[81] DS modified Zn_3/Al-LDH was refluxed in 100 mL xylene for 24 hours under flowing N_2. A sample of 2.0 g PS was added into the Zn_3/Al-DS^--LDH suspension. After stirring for 3 min at 140 °C, the mixture was added into 300 mL ethanol for rapid precipitation. The precipitate was filtered and dried at 100 °C under vacuum for 2 days. The results showed that PS composites containing fully exfoliated Zn_3/Al-LDH can be prepared when the LDH concentration was <10 wt%. This was also the first report to use the X-ray diffraction at 2θ = 60°, indexed as the *110* Bragg reflection (Figure 6c), in a hexagonal lattice with a 3R stacking sequence of sheets, to determine the preservation of layered framework in the delaminated colloids.

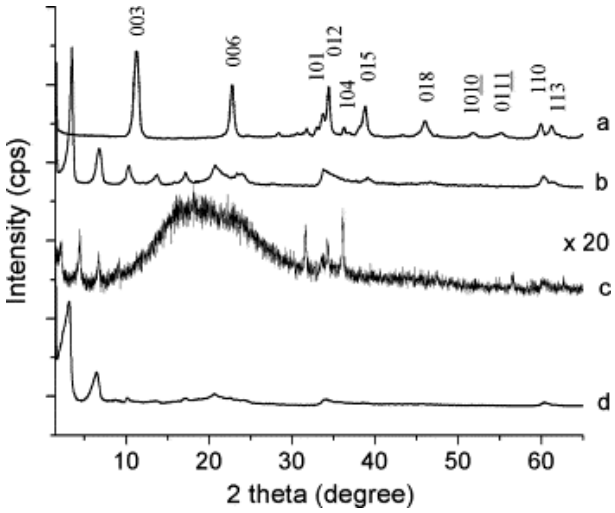

Figure 6. XRD patterns of (a) solid Zn_3/Al-Cl^--LDH, (b) solid Zn_3/Al-DS^--LDH, (c) colloidal suspension of Zn_3/Al-DS^--LDH in xylene, (d) solid Zn_3/Al-DS^--LDH reassembled by evaporating xylene.[81] Reproduced with permission from reference 81. Copyright 2005 Elsevier Inc.

It was reported that partially DS^- modified Mg_3/Al-NO_3^--LDH could be exfoliated by direct melt intercalation of LDH by linear low density polyethylene (LLDPE) to prepare polymer/LDH nanocomposites, in which the load of LDH can be as high as 10 wt%.[82] Because DS^- anions are much larger than nitrate anions, they produced sufficient voids in the interlayer space so that LLDPE chains can penetrate more easily during melt intercalation. Later, Chen et al.[83] extended this method to Mg_3/Al-LDH with another polymer. Mg_3/Al-DS^--LDH can be exfoliated by refluxing in polyethylene-grafted-maleic anhydride (PE-g-MA) and xylene. The resultant nanocomposite showed a higher thermal stability than the pure PE-g-MA in the temperature range of 370 to 500 °C. Furthermore, Chen et al.[83, 84] reported an advanced exfoliation system: a pre-synthesized $Zn_3Al(OH)_8(C_{12}H_{25}SO_4^-)$ (i.e., Zn_3/Al-DS^--LDH) was exfoliated by refluxing the above Zn_3/Al-DS^--LDH powders in a xylene solution containing a desired amount of LLDPE with stirring under a N_2 atmosphere for 24 h.

2.1.4 Exfoliation in formamide

Later on, Hibino and Jones[85] first reported the delamination of LDHs in formamide following the same idea of creating a desirable interlayer environment to uptake a large amount of solvent, resulting in exfoliation. They investigated amino acid anion intercalants and polar solvent systems. Amino acids including glycine, serine, and L-aspartic acid as interlayer anions of Mg_n/Al_k-LDHs with different *n : k* ratios (2:1, 3:1, 4:1) and polar solvents of water, ethanol, acetone, formamide, ethylene glycol, and diethyl ether were studied as dispersants. They managed to directly prepare amino acid containing LDHs through an *in situ* intercalation method instead of through an anion exchange method. Of all combinations, the glycine and formamide led to the optimum result. Rapid exfoliation occurred when stirring 0.03 g of Mg_3/Al-glycine-LDHs in 10 mL formamide within a few minutes. Figure 7 shows the XRD patterns of the exfoliated Mg_3/Al-LDHs containing glycine in formamide.

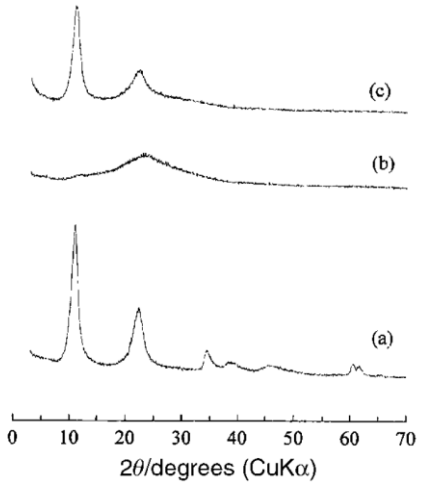

Figure 7. XRD patterns for Mg_3/Al-Glycine-LDHs (a) after preparation and drying in air, (b) 1:1 mixture with formamide indicating absence of LDHs basal diffractions, and (c) of a material obtained by repeated addition of droplets of a completely delaminated mixture.[85] Reproduced with permission from reference 85. Copyright 2001 The Royal Society of Chemistry.

It was noted that for the Mg_3/Al and Mg_4/Al-Glycine/LDHs ratio, up to 3.5 g of LDHs could be delaminated per liter of formamide and the colloidal solution was stable for at least 3 months. However, the Mg_2/Al-Glycine-LDHs only partially delaminated even after the addition of 20 mL formamide. The authors proposed that the attractive interactions caused by the strong hydrogen bonding between the intercalated surfactant and the dispersants as well as between the dispersant molecules themselves would lead to the penetration of a large amount of dispersant and hence leading to exfoliation. Later in 2004, Hibino[86] expanded the investigation of delaminating amino acid containing M^{2+}/Al-LDHs including Ni_3/Al-, Zn_3/Al-, Co_3/Al-, and Mg_3/Al-LDHs in formamide.

Similar approaches were used by Wypych et al.[87] to study the immobilization of porphyrins in exfoliated Mg_3/Al-LDH obtained in formamide. Their result showed that glycinate anions continued to be intercalated and the iron porphyrin anions were adsorbed at the surface of the LDHs crystal layers. Li et al.[88] reported that the exfoliated Mg_2/Al-Glycine-LDH that was synthesized through a hydrothermal reaction for 10 hours at 120 °C possessed a high thermal stability and maximal crystallite size in *a*, *c* directions. Ugur[89] used a similar method and successfully exfoliated Mg_3/Ga-LDH.

In summary, this category represents the pioneering work to delaminate LDHs: the creation of a desirable interlayer environment enabling an attractive interaction between the large intercalating anions and subsequently adding solvent/dispersant that promotes the delamination of LDHs by uptaking a large amount of solvent/dispersant molecules.

2.2 Exfoliation driven by mechanical forces

In 2005, Li et al.[58] reported the first successful exfoliation of large size Mg_2/Al-NO_3^--LDH by formamide without pre-modifications of LDHs with organic guest anions such as fatty acid salts or amino acids. The exfoliation mechanism was believed to be induced by the replacement of water by formamide because of its carbonyl group can interact with LDHs host layers and the other end of formamide molecule, -NH_2, cannot form a strong interaction with the interlayer anions. During their experiments, Li et al.[58] initially synthesized Mg_2/Al-LDH containing carbonate as interlayer anions based on a literature method.[68, 90] A reaction mixture of $Mg(NO_3)_2{\cdot}6H_2O$, $Al(NO_3)_3{\cdot}9H_2O$ and hexamethylenetetramine was mixed in an autoclave and heated at 140 °C for 24 h, followed by filtration and air dry. Half a gram of this carbonate LDH was further treated with 500 mL of an aqueous solution of $NaNO_3$ (0.75 mol) and HNO_3 (0.0025 mol) to expel interlayer carbonate ions. After one day of reaction, Mg_2/Al-NO_3^--LDH was obtained with a large lateral dimension of ca. 10 μm and a uniform hexagonal shape similar to the carbonate LDH precursor (shown in Figure 8A). A sample of 0.05 g nitrate form LDH was mixed with 100 mL of formamide in a flask, which was tightly sealed after purging with nitrogen gas. The mixture was vigorously agitated by a mechanical shaker at a speed of 170 rpm for 12 h, resulting in a transparent solution without sediment. Atomic force microscopy (AFM) was used to characterize the thickness of the exfoliated LDH nanosheets (Figure 8B). The average thickness of 10 different testing spots is 0.81 ± 0.05 nm, suggesting the presence of a single-layer LDH nanosheet (0.48 nm in thickness theoretically), adsorption of anions as well as formamide of ~0.3 nm and the probable presence of van der Waals radius of hydrogen atoms (0.12 nm).[58]

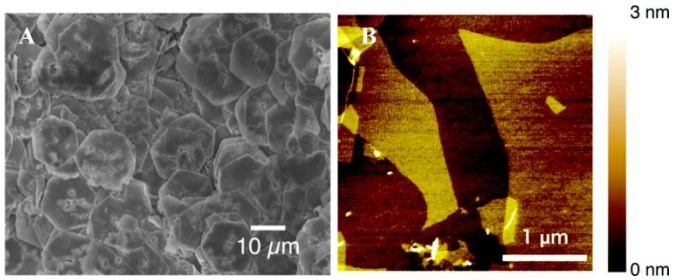

Figure 8. (A). SEM image of the LDH crystals after ion exchange treatment. Some etched pits in the crystals may have formed during the ion exchange process using the acidic solution; (B). Tapping mode AFM image of delaminated LDH nanosheets deposited on a Si wafer substrate.[58] Reproduced with permission from reference 58. Copyright 2005 The American Chemistry Society.

Kentaro et al.[91] adopted this method to prepare highly oriented organic-LDHs hybrid films. The organic modification of Kentaro's method is more versatile for the convenience to convert to other LDHs hybrid films. Later on, Liu et al.[92] expanded the investigation to Co_2/Al-LDHs bearing a variety of anions, including NO_3^-, ClO_4^-, CH_3COO^-, CH_3CHCOO^-, DS^- and $CH_3(CH_2)_7CH{=}CH(CH_2)_7COO^-$, by formamide. Urea hydrolysis synthesized Co_2/Al-LDH (1.0 g) in carbonate form was first ion exchanged into chloride form using 1 L NaCl (1 M) and 3.3 mM HCl. Then Co_2/Al-LDH containing other anions were prepared using the same anion exchange method based on the chloride form of LDH. The results showed that nitrate bearing LDH exhibited the best exfoliation behavior. Complete exfoliation of 0.1 g Co_2/Al-NO_3^--LDH was achieved by mixing with 100 mL formamide after shaking at a speed of 160 rpm for 2 days. After reaction, the resultant clear colloidal suspension showed a

Tyndall effect (Figure 9a). The XRD pattern of the colloidal aggregate obtained after centrifuging the suspension (Figure 9b) showed a noticeable amorphous like halo in the low angular region ($2\theta < 15^{\circ}$) instead of sharp basal diffractions of the Co_2/Al-NO_3^--LDHs, indicating the absence of layered structure. Under the same conditions, other anion intercalated LDHs exhibited different degrees of exfoliation, in which, Cl^-, ClO_4^-, CH_3COO^-, and DS^--LDHs were estimated to be ca. 75%, 50%, 60%, and 95%, respectively. This result suggests that exfoliation in formamide is closely related with the type of interlayer anions.

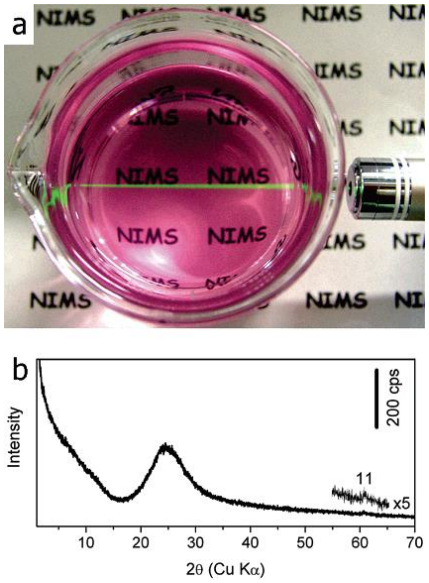

Figure 9. (a) Photograph of a colloidal suspension of exfoliated Co_2/Al-LDH nanosheets. The light beam was incident from the side to demonstrate the Tyndall effect. The LDHs content was 1.0 g/L. (b) XRD pattern of the colloidal aggregate centrifuged from the suspension.[92] Reproduced with permission from reference 92. Copyright 2006 The American Chemistry Society.

In order to understand the detailed exfoliation process, Liu et al. designed several experiments differentiating the volume of formamide (0.25. 0.50 and 0.75 mL) used to exfoliate 0.1 g Co_2/Al-NO_3^--LDH. Figure 10 shows the XRD results of the gel-like samples obtained after centrifuging the resulting mixture from the above mentioned experiments. The XRD pattern (Figure 10a) of the sample in 0.25 mL formamide showed a series basal diffractions in low angular range; based on which the gallery height was estimated to be ca. 6 nm (Figure 10 inset). This high degree of interlayer expansion was attributed to the uptake of a large volume of formamide molecules into the interlayer region, which was defined as the swollen phase. And the basal diffractions of Co_2/Al-NO_3^--LDH were also recognized despite the lowered intensity indicating a small amount of LDHs remained unswollen. When the volume of formamide was increased to 0.5 mL, only the swollen phase was observed and the peaks shifted to lower angles (Figure 10b). When the volume of formamide was increased to 0.75 mL, no basal diffractions were observed in the low angular range and the above observed characteristic diffraction halo in the range of 1-10° was not observed (Figure 10c). This indicated the formation of swollen phase with a very large gallery height (possibly up to tens of nanometers). Upon treatment with a large amount of water, Co_2/Al-NO_3^--LDH can be restored from sample c, indicating the long-range order of the swollen structure with a large volume of formamide in the interlayer region. Only with the assistance of mechanical shearing or ultrasonication could the swollen phase be successfully exfoliated.

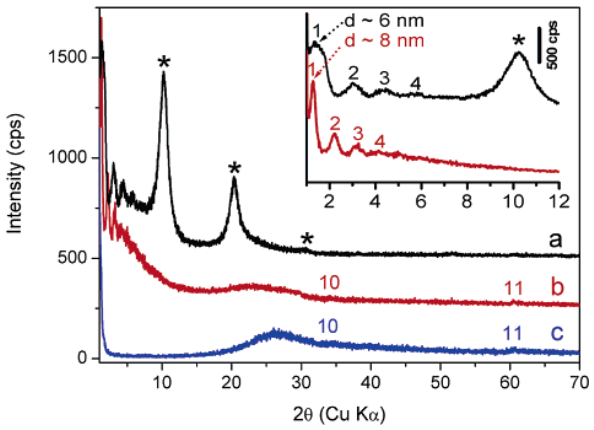

Figure 10. XRD patterns of the gel-like samples obtained by mixing 0.1 g of Co_2/Al-NO_3^--LDH powders with different volumes of formamide: (a) 0.25, (b) 0.50, and (c) 0.75 mL. (Insets) Enlarged view of patterns a and b in the low angular region. The peaks marked by asterisk indicate the basal diffraction series related to the starting Co_2/Al-NO_3^--LDH. The numeral at each peak shown in the inset designates the order of basal diffractions for the swollen phases.[92] Reproduced with permission from reference 92. Copyright 2006 The American Chemistry Society.

Based on the above experimental results, Liu et al.[92] proposed that the exfoliation follows two separate processes (Figure 11): (1) rapid swelling and (2) subsequent slow exfoliation. The swelling is a quick reaction, but the delamination of the highly swollen phase is a progressive process with the assistance of continuous shaking. This process is very similar to the exfoliation of some other layered materials such as layered titanates and manganese oxide.[93-95] Thus the mechanism is believed to be universal.

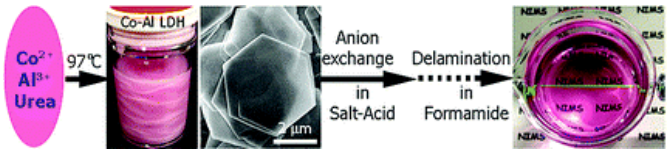

Figure 11. Schematic illustration of the exfoliation process of LDHs in formamide.[92] Reproduced with permission from reference 92 Copyright 2006 The American Chemistry Society.

Liu et al.[96] expanded the exfoliation method to transition metal-bearing LDHs. Well crystallized binary LDHs such as Zn_2/Al and Ni_2/Al-LDHs and ternary LDHs including Zn_n/Co_l/Al_k-LDHs with different n : k : l ratios (1:1:1, 4:1:2.5, 1:4:2.5) can be synthesized via the urea hydrolysis method. The synthesized LDHs were exfoliated in formamide after being ion exchanged with NO_3^-. Similarly, Abellan et al.[97] exfoliated Ni/Fe-NO_3^--LDH in formamide at a concentration of 1 g LDH/L formamide under vigorous stirring for 3 days with 3 intervals of 20 min periodical ultrasonication.

Wu et al.[98] reported the exfoliation of Mg_3/Al-NO_3^--LDH in formamide by ultrasonication in successive intervals of 30 min until the turbidity of the solution became constant. Up to 40 g LDH/L formamide can be exfoliated and LDH gels formed at a concentration of 10 g/L or above. The AFM characterization of the exfoliated LDH nanosheets showed that a large portion of the LDH was delaminated into single- or double-layers (0.7-1.4 nm in thickness) (Figure 12). The nanosheets possessed disk-like shapes with a diameter of ca. 20-40 nm.

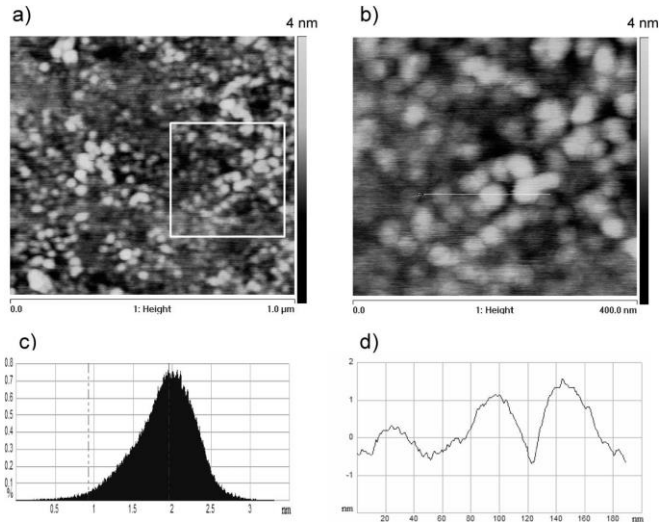

Figure 12. AFM images (tapping mode) of the exfoliated Mg_3/Al-NO_3^--LDH in formamide (0.1 g/L) deposited on a mica substrate. (a) Height image over a scanning area of 1000 × 1000 nm²; (b) height image of the same sample over the marked scanning area of 400 × 400 nm²; (c) depth histogram showing a maximum at 2 nm over the marked area; (d) section profile along the marked white line, showing single and double layers of exfoliated LDH.[98] Reproduced with permission from reference 98. Copyright 2005 The Royal Society of Chemistry.

In 2007, Ma et al.[99] first reported the synthesis of $Co_{2/3}$/$Fe_{1/3}$-LDH with oxidative intercalation by iodine in chloroform. The iodine was used as an oxidant to transform the precursor brucite like Co^{2+}-Fe^{2+} hydroxide into $Co_{2/3}$/$Fe_{1/3}$-LDH and I^- was intercalated in the interlayer region. After an ion exchange process, $Co_{2/3}$/$Fe_{1/3}$-ClO_4^--LDH was obtained. A sample of 0.1 g of $Co_{2/3}$/$Fe_{1/3}$-ClO_4^--LDH was exfoliated into nanosheets in 100 mL formamide by ultrasonicating the mixture for 30 min.

In 2008, Ma et al.[100] explored the same topochemical synthesis method to prepare monometallic Co_n/Co_k-LDHs. β-$Co(OH)_2$ was partially oxidized into a Co_n/Co_k-LDHs with a Co^{2+}:Co^{3+} ratio of 2:1 by intercalating bromine (Br_2). The Br^- bearing Co_n/Co_k-LDHs was then ion exchanged by ClO_4^- to obtain ClO_4^- containing Co_n/Co_k-ClO_4^--LDHs, which was subsequently exfoliated by mixing with formamide followed by an ultrasonication treatment. After exfoliation, positively charged $Co(OH)_2$ nanosheets were obtained. Later on, Liang et al.[101] reported the exfoliation of $Co_{(1-x)}$/Ni_x-LDHs with various Co/Ni ratios through a similar method. Brucite-like $Co^{2+}_{(1-x)}$/Ni^{2+}_x hydroxides were oxidized into $Co_{(1-x)}$/Ni_x-LDHs by oxidative intercalation of Br_2 to obtain $Co_{(1-x)}$/Ni_x-Br^--LDHs, which was ion exchanged into $Co_{(1-x)}$/Ni_x-NO_3^--LDHs. Exfoliation was achieved after mixing 0.05 g $Co_{(1-x)}$/Ni_x-NO_3^--LDHs with 100 mL formamide and shaking at a speed of 170 rpm for 24 h.

However, the LDH nanosheets exfoliated in formamide tend to restack upon water treatment (Figure 13).[58] This phenomenon clearly limits the application of LDH nanosheets exfoliated in formamide. Kang et al.[102] reported that after three cycles of water washing can remove virtually all the formamide in the colloidal solution as evidenced by the formation of a halo at a 2θ region of 25˚-45˚ (Figure 13d). Co-assembly of LDH nanosheets with carboxymethyl cellulose was found to be able to stabilize LDH nanosheets in aqueous suspension, preventing them from flocculation after all formamide was replaced by water.

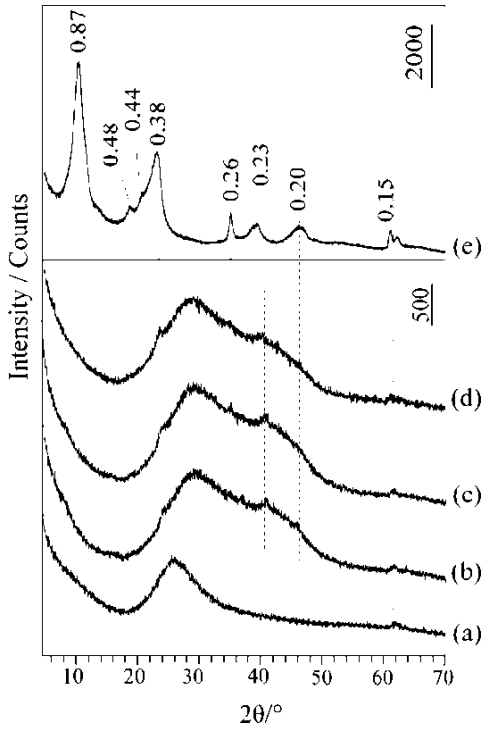

Figure 13. XRD patterns of (a) colloidal suspension of LDHs in formamide, and the samples (b-d) water-washed 1, 2, and 3 times respectively, and (e) dried; d-values in nanometers.[102] Reproduced with permission from reference 102. Copyright 2009 The American Chemistry Society.

In 2013, Chen et al.[103] followed the same idea of utilizing the carbonyl group of a dispersant to interact with the LDHs layers to replace the interlayer water molecules. Unlike Ma et al.[57, 58, 99, 100] who used formamide as exfoliation dispersant, Chen et al. explored L-asparagine, which has a similar structure as formamide. The exfoliation of the Co_2/Al-LDH, which was prepared and anion exchanged following a previous reported method,[33] was achieved by dispersing 0.1 g of Co_2/Al-NO_3^--LDH in L-asparagine saturated aqueous solution (5 g L-asparagine in 100 mL water at 45 ˚C), followed by ultrasonication and purging with nitrogen gas, and vigorous oscillation at 45 ˚C for 48 h. After that, the mixture was stored at 4 ˚C overnight to insure most L-asparagine was crystalized and precipitated at the bottom of the container. The AFM characterization of the obtained nanosheets showed an average height of ca. 8 nm, which indicated the exfoliation was incomplete.

A simple method to determine the exfoliation degree of nitrate and glycine intercalated LDHs in formamide was reported by Wang et al.[104] XRD was used as the main characterization tool. Figure 14a and b shows the XRD patterns of the exfoliated Mg_2/Al-NO_3^--LDH gels in formamide. At a concentration below 100 g/L, the typical basal diffraction of LDHs layered structures could not be observed. The absence of the basal diffraction suggested that the LDHs host sheets were not in parallel to induce diffractions, suggesting that the LDHs was completely exfoliated into individual nanosheets. However, at a concentration of 120 g/L, the basal diffraction started to appear, which indicated the presence of layered structure. The authors thus proposed that LDHs cannot be completely exfoliated if its concentration in formamide was too high. Figure 14c shows the plate-like morphology of the exfoliated Mg_2/Al-LDH nanosheets, which was different from the flower-like morphology of the original LDHs particles (Figure 14d).

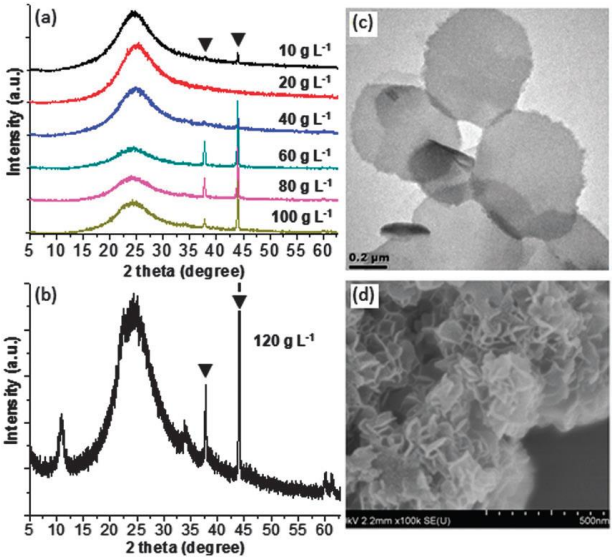

Figure 14. XRD patterns of the delaminated Mg_2/Al-NO_3^--LDH dispersion gels at different LDHs concentrations: (a) from 10 to 100 g/L, (b) 120 g/L, (c) HR-TEM image of the delaminated Mg_2/Al-NO_3^--LDH, and (d) SEM image of Mg/Al-NO_3^--LDH. (▼) sample holder.[104] Reproduced with permission from reference 104. Copyright 2014 The Royal Society of Chemsity.

2.3 Exfoliation in water

The very first report on the nearly exfoliation of LDHs in water was reported by Gardner et al.[105] "Nearly transparent colloidal solutions of LDHs particles" were obtained by hydrolysis of Mg_3/Al-CH_3O^--LDH in water at room temperature, though the term "exfoliation" was not used in their paper. Hibino et al.[106] developed the exfoliation of Mg_n/Al_k-$CH_3CHOHCOO^-$-LDHs with n : k molar ratio varies from 2:1, 3:1 to 4:1. During the entire reaction process, decarbonated water was used as the only solvent and exfoliation agent. Mg_n/Al_k -$CH_3CHOHCOO^-$-LDHs was synthesized by titrating magnesium and aluminum lactate into DL-lactic acid (a mixture of the two chiral lactic acids in equal amounts) solution pre-adjusted to pH 10 by adding NaOH (Figure 15a). The lactic acid solution was maintained at pH =10 during the titration process by adding NaOH. Then, the resulting Mg_n/Al_k-$CH_3CHOHCOO^-$-LDHs was centrifuged and washed, and finally stored in water. After a certain amount of time (10-20 g/L solution typically requiring 3-5 days), the opaque suspension of the stored Mg_n/Al_k-$CH_3CHOHCOO^-$-LDHs became transparent. Figure 15b shows the AFM image of the sample on mica. An average thickness of large sheets (100-150 nm in diameter) was ca. 2.5 nm, while smaller sheets generally showed a thickness of 0.55-0.95 nm.

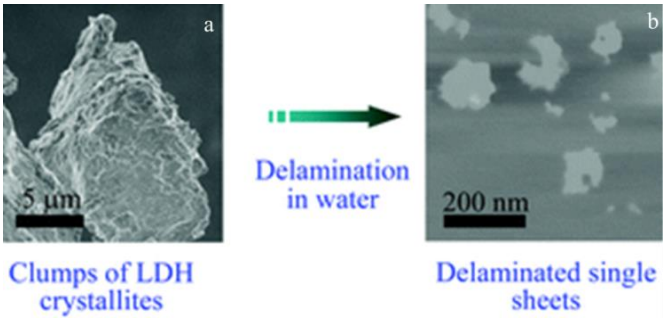

Figure 15. SEM image of Mg_3/Al-$CH_3CHOHCOO^-$-LDH before delamination (a) and AFM image of the delaminated Mg_3/Al-$CH_3CHOHCOO^-$-LDH sheet on a mica (b).[106] Reproduced with permission from reference 106. Copyright 2005 The Royal Society of Chemistry.

In 2006, Jaubertie et al.[107] exfoliated Zn_n/Al_k-$CH_3CHOHCOO^-$-LDHs (prepared via the same synthesis method as reported by Hibino and coauthors[106] with n : k molar ratio varies from 2:1, 3:1, to 4:1) with the assistance of ultrasonication. Delamination of the Zn_n/Al_k-$CH_3CHOHCOO^-$-LDHs in water or butanol under reflux was unsuccessful. However, the exfoliation of the LDHs was successful in water with ultrasonication treatment. In 2008, San Roman et al.[108] expanded the delamination method into another LDHs, Mg_n/Al_k-$CH_3CHOHCOO^-$-LDHs (with n : k molar ratio varies from 2:1, 3:1, to 4:1) in water with ultrasonication. In 2010, Okudaira et al.[109] reported the exfoliation of a $CH_3CHOHCOO^-$-LDHs in water through a reconstruction method. The titration synthesized Mg_3/Al-LDH was intercalated by lactate through a reconstruction method by immersing 500 °C calcined Mg_3/Al-LDH in sodium lactate solution. A sample of 0.5 g Mg_3/Al-$CH_3CHOHCOO^-$-LDH was redispersed in sodium lactate solution and it was exfoliated after aging for 2-3 weeks as suggested by XRD. Figure 16a shows the disappearance of the basal diffractions, which suggested the achievement of a successful exfoliation, while Figure 16b shows the restacking of the exfoliated nanosheets after drying at 80 °C. The AFM characterization evidenced that the delaminated nanosheets were 4-8 nm in height and 50-150 nm in diameter.

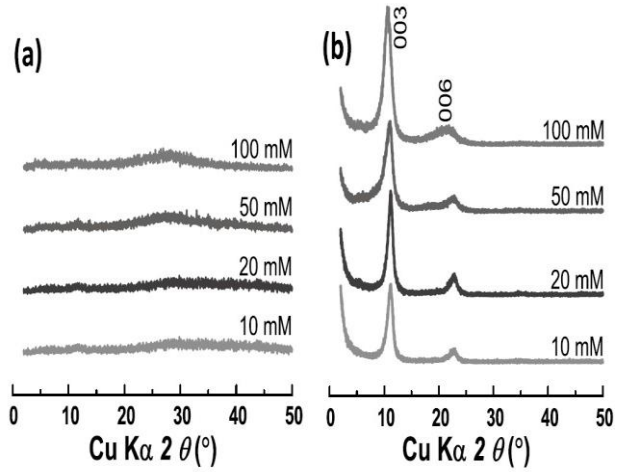

Figure 16. XRD patterns of the re-dispersed and gelated sample of the $CH_3CHOHCOO^-$-LDH in water: (a) before drying and (b) after drying at 80 °C.[109] Reproduced with permission from reference 109. Copyright 2010 Japan Society of Colour Material.

At the same time, Manohara et al.[110] delaminated $Ni_{0.57}/Al_{0.4}$-$CHOO^-$-LDH in water. A $Ni_{0.57}/Al_{0.4}$-$CHOO^-$-LDH was prepared through formamide hydrolysis at 150 °C for a day. A sample of 0.1 g as prepared LDH was mixed with 100 mL decarbonated water. The mixture was then stirred for 96 h and diluted to ca. 200 mL with an ultrasonication treatment for 20 min. The AFM characterization showed that the particles possessed a thickness of 9-12 nm with in lateral dimensions of 100-200 nm.

In 2010, Antonyraj et al.[111] synthesized nitrate containing LDHs without carbonate contamination by a hexamethylenetetramine (HMT) hydrolysis method at 80 °C. The as prepared NO_3^--LDHs was successfully delaminated in water and completely delaminated in formamide. The synthesis of the NO_3^--LDHs was confirmed to be very temperature sensitive and some of their results were not reproductive. A representative synthesis process was to mix 80 mL of 1 M divalent and trivalent metal ions (all nitrate salts) of 2:1 ratio with 120 mL HMT solution in a molar ratio of $[M^{2+} + M^{3+}]$: [HMT] of 1 : 1.5. The mixture was nitrogen purged for 30 min and kept in an oil bath at 80 °C for four days without stirring. The temperature was kept below 80 °C, which resulted in the pH between 5 and 6.5 throughout the reaction. If the temperature was slightly increased (~90 °C), the pH of the solution increased to more than 8, which led to the formation of CO_3^{2-}-LDHs. Exfoliation of the prepared NO_3^--LDHs in water was studied by reacting 2.5 g of wet LDHs immediately after filtration in a hydrothermal reactor, to which 50 mL of water was added and kept at 120 °C for 12 h in nitrogen atmosphere. Exfoliation of the prepared NO_3^--LDHs in formamide was conducted by dispersing 0.05 g of dried LDHs powders in 50 mL formamide where the reaction mixture was sealed after being purged with nitrogen and vigorously agitated by a mechanical shaker at a speed of 150 rpm for two days.

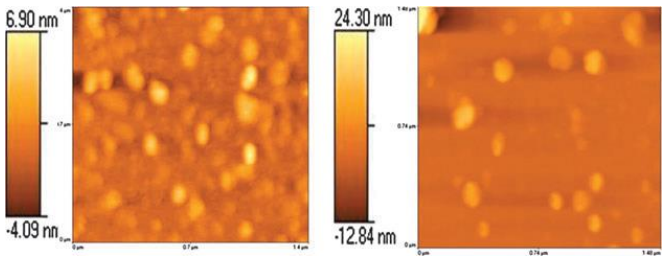

Figure 17. AFM images of Co_2/Al-NO_3^--LDH delaminated in (a) formamide and (b) water.[111] Reproduced with permission from reference 111. Copyright 2010 The Royal Society of Chemistry.

The AFM images (Figure 17) showed that the Co_2/Al-LDH was exfoliated in formamide and water. A similar sheet thickness ranging from 2-10 nm in both formamide and water was determined, which suggested that the dispersant did not affect the degree of exfoliation.

2.4 Other exfoliation methods

Several methods use either low temperature or electrostatic interactions between LDHs layers and intercalated anions, which do not fall into our previous categories. Thus, they are reviewed separately below.

2.4.1 Exfoliation by electrostatic repulsion

In 2007, Hou et al.[72] reported the exfoliation of a Ni_4/Fe-LDH intercalated with 11-aminoundecanoic acid (AUA) (Ni_4/Fe-$NH_2(CH_2)_{10}COO^-$-LDH) as pillared species by an electrostatic repulsive mechanism between the guest species and the inorganic host layers. The Ni_4/Fe-$NH_2(CH_2)_{10}COO^-$-LDH was synthesized by dissolving 4 g of AUA in 100 mL water, to which a mixed solution (10 mL) of nickel and iron chlorides was added drop by drop at room temperature. The reaction mixture was maintained at pH = 9.4 by adding 1 M NaOH solution. After reaction, the mixture was aged at 60 ˚C for a day. Exfoliation was achieved by stirring the as prepared Ni_4/Fe-$NH_2(CH_2)_{10}COO^-$-LDH in HCl solution with an initial pH value of 2, 3, and 4 for 2 days at room temperature, during which the protonation of the amine group (-NH_2) of the intercalated AUA anions took place. Figure 18 shows the XRD patterns of the LDH stirred in an acid solution with an initial pH of 2, 3, and 4. The sharp basal diffractions of Ni_4/Fe-$NH_2(CH_2)_{10}COO^-$-LDH gradually diminished with a decreasing pH value (Figure 18a and b) and finally disappeared at the initial pH = 2 (Figure 18c), which indicated exfoliation. The exfoliation was confirmed by the AFM characterization, which showed that the exfoliated nanosheets possessed a diameter of ca. 100 nm and an average thickness of ca. 2 nm.

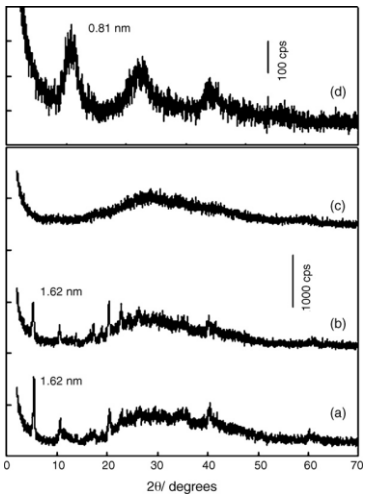

Figure 18. XRD patterns: (a)-(c) exfoliated samples in acid suspensions with an initial pH of 4, 3, and 2, respectively, and (d) restacked Ni_4/Fe-LDH.[72] Reproduced with permission from reference 72. Copyright 2008 Elsevier Inc.

2.4.2 Exfoliation at low temperatures

Wei et al.[112] reported the exfoliation of Zn_7/Al_3-LDH using NaOH/urea aqueous solution at low temperatures by taking advantage of a special property of alkali and urea aqueous solution system at low temperatures that can dissolve cellulose with strong inter- and intra- molecular hydrogen bonding. In their experiments, 5 wt% hydrothermally synthesized LDH was stirred vigorously in 6-9 wt% NaOH and 10-15 wt% urea mixed aqueous solution for 3 min, which was precooled at –10 ˚C. The obtained LDH nanosheets were of an average thickness of ca. 0.6 nm corresponded to single-layer LDHs thickness. The exfoliation mechanism study revealed that NaOH and urea can form hydrates at low temperatures. The NaOH hydrate was intercalated into the LDH and attached onto the host layers to break the hydrogen bond network between the LDH layers and formed new hydrogen bond network between the NaOH hydrate and the hydroxyl groups on LDH layers. The urea hydrate can be easily self-assembled at the surface of NaOH hydrate bonded LDH layer surface to prevent the aggregation of LDH nanosheets. The combination of the NaOH and urea solution system at low temperatures destroyed the hydrogen bonding in-between the LDH layers, leading to the exfoliation of LDH and stabilization of the exfoliated colloidal nanosheets, as shown in Figure 19.

Figure 19. Schematic diagram of exfoliation of LDHs in precooled NaOH/urea aqueous solution.[112] Reproduced with permission from reference 112. Copyright 2014 The Royal Society of Chemistry.

2.5 Direct synthesis methods

Bottom-up direct synthesis of LDH nanosheets is an attractive route due to its relative facile process where the pre-synthesis of layered LDHs can be omitted. Various concepts including chemical approaches to create “microreactors” utilizing microemulsion method as well as to inhibit the growth of the layers by a layer growth inhibitor, mechanical approaches to apply laser beam on metals in aqueous solution, and to establish a quick mixing environment by a special reactor have been explored.

2.5.1 Chemical methods

In 2005, Hu et al.[113] reported a facile one step synthesis of LDHs single-layer nanosheets in a reverse micro-emulsion system. The traditional titration method (where magnesium salt and aluminum salt are co-precipiated at pH ≥ 10) was adopted in an oil phase (isooctane) with SDS as surfactant and 1-butanol as co-surfactant to prepare LDHs single-layer nanosheets. As shown in Figure 20, in the system, aqueous droplets containing the reactants were surrounded by DS^- groups in the oil phase. These droplets acted as nano-reactors to confine space and nutrients for the growth of LDHs platelets, providing a way to control the size of the LDHs platelets both in diameter and thickness. An representative preparation example is as follows: 18.34 g $Mg(NO_3)_2{\cdot}6H_2O$ and 9.00 g $Al(NO_3)_3{\cdot}9H_2O$ was dissolved in 30 mL water to prepare solution A. Solution B was prepared by dissolving 6.97 g $NaNO_3$ and 4.8 g NaOH in 30 mL water. A 4 M NaOH solution was used to adjust the pH value of the system. Solution A (1.73 g) was added drop by drop into 50 mL isooctane solution, which contained 0.72 g SDS and 0.76 g 1-butanol to form a clear system. Then, 1.25 g solution B and 0.47 g NaOH solution were similarly dispersed to make a clear solution. This solution was then added drop by drop into the former system. The reaction mixture turned to be slightly translucent and became milky when heated at 75 °C in an oil bath for 24 hours.

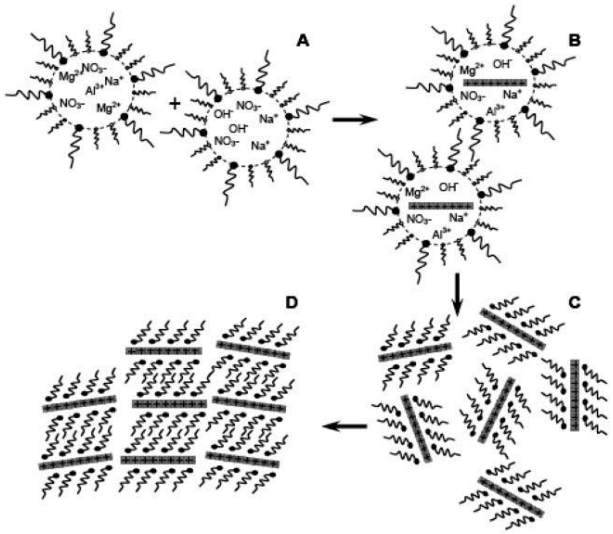

Figure 20. Schematic representation of the nucleation and growth of LDHs platelets.[113] Reproduced with permission from reference 113. Copyright 2006 The Royal Society of Chemistry.

The obtained LDH nanosheets were characterized by AFM.[113] Figure 21a shows a representative topology of isolated oval objects with a diameter of ca. 40 nm. The height profiles are presented in Figure 21b, which show that all the particles have a height of ca. 1.5 nm, corresponding to three monolayers without taking interlayer spacing expanded by DS^- anions into consideration. Considering the presence of DS^- was evidenced by the elemental analysis (not shown here), it indicated that the LDH nanosheets formed in the reverse micro-emulsion had a monolayer structure.

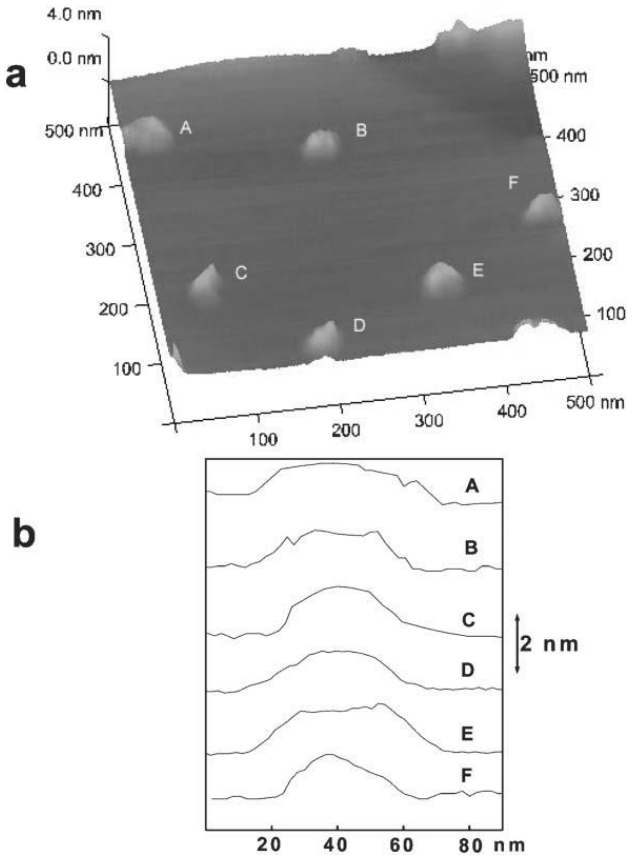

Figure 21. (a) AFM image of the particles synthesized by reverse micro-emulsion method deposited on highly oriented pyrolytic graphite (HOPG) surface; (b) cross-sectional analysis of the labeled particles in (a) showing the dimensional profiles.[113] Reproduced with permission from reference 113. Copyright 2006 The Royal Society of Chemistry.

Later, in order to avoid a complex purification process to remove anionic surfactants that were usually attached onto the surface of LDH nanosheets as counter anions obtained during a surfactant based reverse micro-emulsion process, Bellezza et al.[114] used cationic surfactant based reverse micro-emulsion method to prepare LDH nanosheets without the surfactant removal issue.

Yan et al.[115] reported another method to prepare LDH nanosheets in aqueous solution in 2011. The use of a high concentration of H_2O_2 was the key to prepare the LDH nanosheets. $Mg(NO_3)_2$, $Al(NO_3)_3$ and urea were dissolved in 30 mL 30 wt% H_2O_2 (Mg^{2+} 0.01 M, Al^{3+} 0.005 M and urea 0.05 M). Then the reaction mixture was transferred into a Teflon lined hydrothermal reactor and heated at 150 °C for 24 h. The authors believed that during the synthesis, part of H_2O_2 and O_2 could be positioned in the gallery of LDHs layers. The rapid decomposition of H_2O_2 catalyzed by LDHs was hypothesized as the major cause to exfoliate LDHs by creating a large amount of O_2 that generated violent movements, leading to the separation of LDHs layers (Figure 22A). The AFM image (Figure 22B) showed that the obtained nanosheets had an average thickness of ca. 1.44 nm, corresponding to the theoretical thickness of approximately two LDHs layers (0.76 *2 = 1.52 nm).

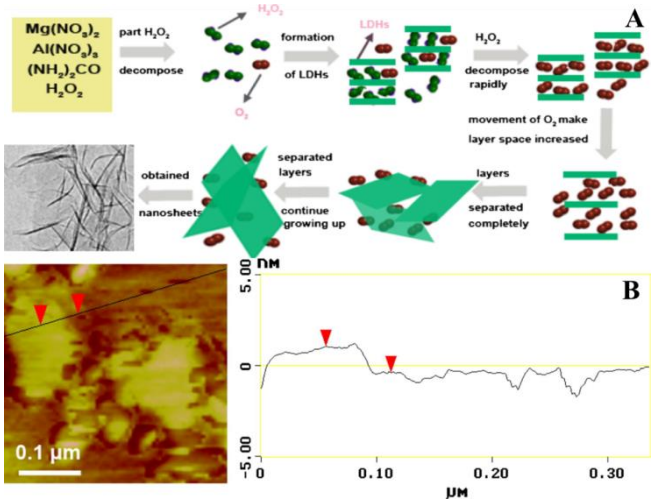

Figure 22. (A) Proposed scheme for the preparation of exfoliated Mg_2/Al-LDH nanosheets; (B) AFM image of synthesized ultrathin sheets.[115] Reproduced with permission from reference 115. Copyright 2012 Elsevier Inc.

Sun and coworkers[45] reported a direct synthesis method to synthesize LDHs single-layer nanosheets in the presence 23 vol% formamide through a co-precipitation route. During the synthesis of LDHs, formamide molecules were adsorbed onto LDHs surface, which prevented the formation of layered structure due to the high dielectric constant of formamide and its preferred interaction with LDHs layer surface. Thus, in the presence of formamide, LDHs single-layer nanosheets were prepared, while without the presence of formamide, layered LDHs was synthesized (Figure 23a).

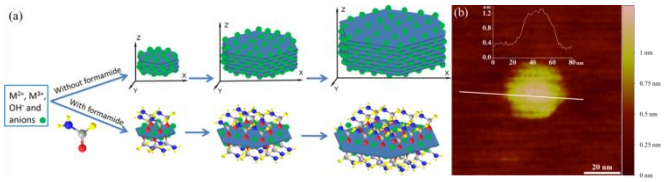

Figure 23. (a) Direct growth of LDH single-layer nanosheets with the assistance of layer growth inhibitors (not drawn to scale); (b) AFM image of a pseudohexagonal Mg_4/Al-LDH nanosheet.[45] Reproduced with permission from reference 45. Copyright 2015 The Royal Society of Chemistry.

The AFM image (Figure 23b) of the prepared LDHs single-layer nanosheets indicated an average layer thickness of ca. 0.8 nm of one metal hydroxides layer with surface adsorbed anions and formamide molecules. The facile method can be potentially used for large scale production due to its simplicity and low operational requirements.

Further study by this group[116] indicated that with increasing volume percentage of formamide present in the reaction system, LDHs single-layer nanosheets can be better prepared (Figure 24A). And it is also clear that LDHs with higher layer charge favors the formation of LDHs single-layer nanosheets (Figure 24 A and B). AFM images showed that Mg_2Al-LDH prepared in 30 vol% formamide showed single-layer feature (Figure 24 C and D).

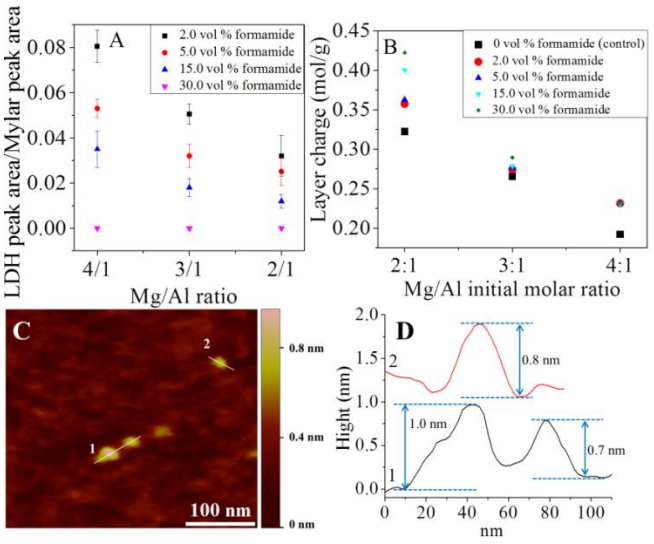

Figure 24. A: LDH characteristic peak to internal reference peak area ratios. B: MgAl-LDH layer charge at different Mg/Al formulation molar ratios and formamide concentrations. C: Representative AFM image of Mg_2Al-LDH prepared in 30.0 vol% formamide and the corresponding height profile (D).[116] Reproduced with permission from reference 116. Copyright 2016 The American Chemistry Society.

2.5.2 Mechanical methods

Preparation of LDHs through pulsed-laser ablation (laser wavelength 1064 nm) method has been reported.[117] $Zn_{1.48}$/Al, $Co_{0.96}$/Fe, $Co_{1.07}$/Al, and $Mg_{1.97}$/Fe-LDHs colloidal nanosheets were synthesized by a laser ablation method.[118] The process consisted of two consecutive steps: (1) laser ablation of trivalent metal target in water at room temperature using Q-switched neodymium:yttrium-aluminum-garnet (Nd:YAG) laser; (2) the same laser ablation over a bivalent metal target in the previously prepared trivalent metallic colloid. It took ca. 40 min to synthesize an LDH colloidal dispersion, which contains ca. 10 mg of metal elements ablated from both metal targets in 40 mL of water. The TEM images showed that the $Mg_{1.97}$/Fe, $Co_{0.96}$/Fe, $Co_{1.07}$/Al, and $Zn_{1.48}$/Al-LDHs nanosheets had a thickness of ca. 0.5, 0.48, 0.5, and 1.2 nm, respectively. The $Mg_{1.97}$/Fe and $Co_{0.96}$/Fe-LDHs nanosheets exhibited a rolling-and-folding morphology in conjunction area (Figure 25), while the edges of $Co_{1.07}$/Al and $Zn_{1.48}$/Al-LDHs nanosheets were intensively rolled. The authors hypothesized that the reasons that LDH nanosheets could be prepared was because of the very short reaction time and high laser power, which limited the carbonates from being incorporated into the LDHs layers.

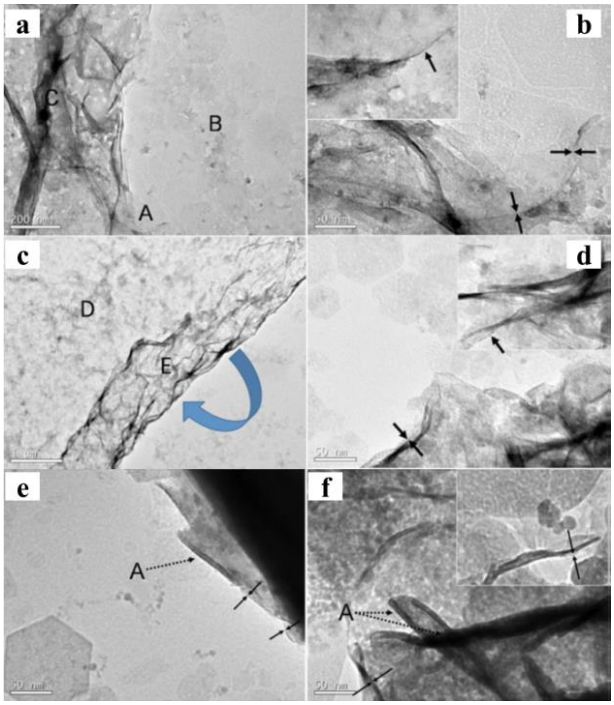

Figure 25. TEM images of $Mg_{1.97}$/Fe and $Co_{0.96}$/Fe-LDHs materials. Scale bars in $Mg_{1.97}$/Fe-LDH images, (a) and (b), represent 200 nm and 50 nm, respectively. Scale bars in $Co_{0.96}$/Fe-LDH images, (c) and (d), represent 1 μm and 50 nm, respectively. (e) $Co_{1.07}$/Al and (f) $Zn_{1.48}$/Al-LDHs nanosheets. The dotted arrows marked by symbol "A" indicate the edges of the nanosheets seriously rolled because of the instability of the edges of the free-standing ultrathin LDHs layers. Both scale bars represent 50 nm in (e) and (f). Insets in images (b), (d), and (f) display the corresponding side views.[118] Reproduced with permission from reference 118. Copyright 2010 American Institute of Physics.

A T-type micro-channel reactor was designed to prepare LDH nanosheets without using any surfactants. Pang et al.[119] adopted the titration method in the T-type micro-channel reactor in water for the synthesis. A mixed salt solution (contained Mg^{2+} and Al^{3+} cations) and an alkali solution contained $NH_3 \cdot H_2O$ were pumped into the reactor through two inlets each at a flow rate of 20 mL/min. The resulting LDH nanosheets were of a thickness of ca. 0.68-1.13 nm, which corresponded to 1-2 brucite-like layers and a diameter of 20-30 nm as evidenced by the AFM characterization (Figure 26)

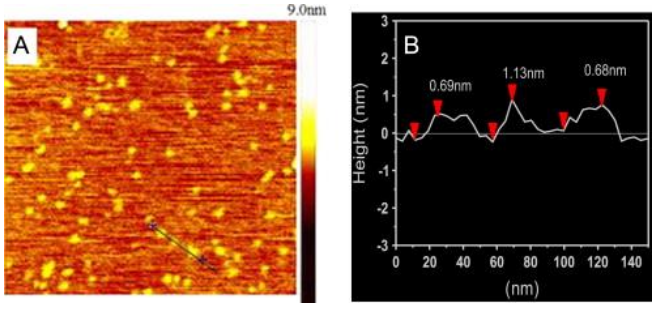

Figure 26. (A) AFM image and height scale of the LDH nanosheets, and (B) sectional analysis along the black line marked in (A).[119] Reproduced with permission from reference 119. Copyright 2014 Elsevier Inc.

The conventional process to exfoliate LDHs consists of two steps: (1) preparation of layered LDHs through various methods; (2) Intercalation of large molecules to induce

exfoliation. Proper solvent selection is pivotal towards a complete delamination.[74, 86] Mechanical agitation to drive exfoliation and reflux to replace interlayer water molecules are adopted in the exfoliation process. Direct growth of LDHs single-layer nanosheets has focused on limiting the reaction time, space, and the amount of reactant.[113, 119] Different LDHs exfoliation methods/direct growth methods are summarized in Table 1.

Chem Soc Rev

Review ARTICLE

Table 1. A summary of LDHs exfoliation/direct growth methods.

No.	Layered double hydroxides	Intercalant /interlayer anion	Dispersant	Process	Stability	Exfoliation state/degree	Reference
1	Zn_2/Al-LDH	DS^-	Butanol	Refluxing at 120 ˚C for 16 hours	At least 8 months	Fully exfoliated	Adachi-Pagano 2000[74]
2	Li/Al_2-LDH	OS^-, DS^-, OBS^- and DBS^-	Butanol	Refluxing at 120 ˚C for 16 hours	OBS and DBS stable for either 12 hours or 7 days depending on gibbsite size	OS^- and DS^- do not work While OBS and DBS work and less than example 1	Singh et al 2004[75]
3	Mg_3/Al-LDH and Mg_4/Al-LDH	Glycine	Formamide	Stirring for a few minutes	At least 3 month	Fully exfoliated	Hibino and Jones 2001[85]
	Mg_2/Al-LDH			Stirring	Not specified	Partially exfoliated	
4	$Mg_{0.67}/Al_{0.33}$-LDH, $Co_{0.67}/Al_{0.33}$-LDH, $Ni_{0.67}/Al_{0.33}$-LDH, $Zn_{0.67}/Al_{0.33}$-LDH	DS^-	Toluene	Stirring followed by 5 min of ultrasonication	Not specified	Successful*	Naik et al. 2011[78]
5	$Mg_{0.71}Al_{0.29}$-LDH	DS^-	CCl_4	30 min ultrasonication and 2 hrs equilibrium time	Not specified	Successful*	Jobbágy et al. 2004[77]
6	Mg_2/Al-LDH	DS^-	HEMA[e]	High shear stirring at 2500- 3000 rpm for 20 min at 70 °C	Several weeks	Almost complete	O'Leary et al. 2002[80]
7	Zn_3/Al-LDH	DS^-	polystyrene	Pre-refluxed in xylene for 24 then add PS and stirring for 3 min at 140 °C	Not specified	Complete*	Qiu et al. 2005[81]
8	$Mg_{0.65}/Al_{0.33}$-LDH	NO_3^-	Formamide	LDHs was mixed with pure formamide which was tightly sealed after purging with N_2. The mixture was vigorously agitated by a mechanical shaker at a speed of 170 rpm for 12h	Not specified	Complete*	Li et al. 2005[58]
9	$Co_{0.67}/Al_{0.33}$-LDH	NO_3^-, ClO_4^-, acetate, lactate, DS^- and oleate	Formamide	Mixing 0.1 g of chosen anion bearing LDHs with 100 mL formamide and then apply vigorous shaking at 160 rpm for 2 days	Very stable	Complete*	Liu et al 2006[92]
10	$M(II)_{0.67}/Al_{0.33}$-LDHs and $[M(II)\text{-}M'(II)]_{0.67}/Al_{0.33}$-LDHs	NO_3^-, ClO_4^-, lactate, DS^- and so on	Formamide	Mixing 0.1 g of chosen anion bearing LDHs with 100 mL formamide and then apply vigorous shaking at 160 rpm for 2 days	Very stable	Zn-containing LDHs: 40% Co-Al and Ni-Al LDHs are complete	Liu et al 2007[96]
11	$Ni_{0.75}/Fe_{0.25}$-LDH	NO_3^-	Formamide	Mixing 0.1 g of LDHs with 100 mL formamide then vigorous stirring at 600 rpm for 3 days with 3 intervals of 20 min periodically sonication	stable	Successful*	Abellan et al. 2010[97]

12	Mg_3/Al-LDH	NO_3^-	Formamide	Ultrasonication in successive intervals of 30 min until the turbidity of the solution becomes constant	stable	Not completely	Wu et al. 2005[98]
13	$Co_{2/3}/Fe_{1/3}$-LDH	ClO_4^-	Formamide	Mixing 0.1 g of LDHs with 100 mL formamide then ultrasonication for 30 min	Stable	Not provided	Ma et al. 2007[99]
14	$Co_{2/3}/Co_{1/3}$-LDH	ClO_4^-	Formamide	Mixing 0.1 g of LDHs with 100 mL formamide then ultrasonication for 30 min	Stable	Not provided	Ma et al. 2008[100]
15	Co^{3+}_{1-x}/Ni^{2+}_x-LDHs	NO_3^-	Formamide	Mixing 0.05 g of NO_3^- intercalated Co^{3+}_{1-x}/Ni^{2+}_x-LDHs with 100 mL formamide and then apply vigorous shaking at 170 rpm for 24 h	Stable	Not provided	Liang et al. 2009[101]
16	Mg_n/Al_k-LDHs (n : k = 2:1, 3:1, and 4:1)	Lactate	Water	Synthesis lactate containing LDHs and wash then store it in water (concentration can be as high as 10-20 g/L).	Stable	Not provided	Hibino et al. 2005[106]
17	Zn_n/Al_k-LDHs (n : k = 2:1, 3:1, and 4:1)	Lactate	Water	Prepare lactate containing LDHs and exfoliation with the assistance of ultrasonication	Stable	Not provided	Jaubertie et al. 2006[107]
18	Mg_n/Al_k-LDHs (n : k = 2:1, 3:1, and 4:1)	Lactate	Water	Prepare lactate containing LDHs and exfoliation with the assistance of ultrasonication	stable	Not provided	San Roman et al. 2008[108]
19	Ni_4/Fe-LDH	AUA	HCl	50 mg LDHs was stirred in 25 mL HCl of initial pH value of 2	Not specified	Successful*	Hou et al. 2008[72]
20	Ni_2/Al and Co_2/Al-LDH	NO_3^-	Water and formamide	Exfoliation in water was done by reacting 2.5 g of wet-LDHs immediately after filtration in a hydrothermal reactor to which 50 mL of water was added and kept at 120 °C for 12 h in nitrogen atmosphere. Total delamination in formamide was done by mixing 0.05 g dried LDHs powder with 50 mL formamide and the reaction mixture was sealed after purged with nitrogen and vigorously agitated by a mechanical shaker at the speed of 150 rpm for two days	Not specified	Successful* in water and complete in formamide	Antonyraj et al. 2010[111]

21	Zn_7/Al_3-LDH	Not specified	NaOH and urea precooled at minus 10 °C	Stirring a certain amount of Zn/Al-LDHs in NaOH and urea solution system for 3 min.	Stable	Successful*	Wei et al. 2014[112]

Direct synthesis methods

No.	Layered double hydroxides	Interlayer anion	Reaction solvent system	Process	stability	Exfoliation state	Reference
1	Mg_2/Al-LDH	DS^-	Isooctane with SDS and 1-butanol	LDHs monolayers were synthesized in a microemulsion system using a tradition titration method as detailed in the main text.	Stable in acrylate monomers	Successful*	Hu et al. 2006[113]
2	Mg_2/Al-LDH	NO_3^-	30 wt% H_2O_2	$Mg(NO_3)_2$, $Al(NO_3)_3$ and urea were dissolved in 30 mL 30 wt% H_2O_2 making the concentration of Mg^{2+} 0.01 M, Al^{3+} 0.005 M and urea 0.05 M. Then the reaction mixture was transferred into a Teflon liner hydrothermal reactor and heated at 150 °C for 24 hr	Stable	Successful*	Yan et al. 2012[115]
3	$Zn_{1.48}$/Al, $Co_{0.96}$/Fe, $Co_{1.07}$/Al, and $Mg_{1.97}$/Fe-LDHs	None	Water	Laser ablation of M (III) and M (II) metals in deionized water	Stable	Not provided	Hur et al. 2010[118]
4	Mg_2/Al-LDH	NO_3^-	Water	A mixed salt solution (containing Mg^{2+} and Al^{3+} cations) and an alkali solution containing $NH_3 \bullet H_2O$ were pumped into the reactor through two inlets each at a flow rate of 20 mL/min.	Stable for ca. 16 h at room temperature in aqueous solution	Successful*	Pang et al. 2014[119]
5	Mg_4/Al-LDH Mg_2/Al-LDH	NO_3^-	Water	LDHs single-layer nanosheets were synthesized in the presence of formamide in a one-step process.	Stable for months at room temperature	Successful*	Yu et al. 2015[45], 2016[116]

*Successful：the cited methods can produce single-layer nanosheets but containing multi-layered LDH as well；Complete：the methods can obtain single-layer LDH nanosheets with virtually no stacked layers.

Chem Soc Rev

Review ARTICLE

3. Applications of LDH nanosheets

LDHs have been widely studied as additives in polymers. However, thanks to its versatile metal cations and interlayer anions composition, new and exciting applications continue to emerge. In this section, we focus on four key applications: (1) LDH nanosheets catalyst as a promising substitute of rare metal oxide for oxygen evolution reaction, (2) LDH nanosheets as a constructing materials for supercapacitors, (3) LDH nanosheets as supports for light emitting instruments, and (4) LDH nanosheets as green flame retardant in polymer composites.

3.1 Catalysts

3.1.1 Oxygen evolution reactions

Recently, attention on LDHs catalyzed oxygen evolution reaction from water is increasing.[120-151] Song et al.[152] observed that various LDHs nanosheet catalysts could enhance oxygen evolution and offer high activity, stability and efficiency compared with the conventional IrO_2 catalyst. By adopting exfoliated $Co_{2/3}/Co_{1/3}$, $Ni_{1/3}/Co_{2/3}$, and $Ni_{3/4}/Fe_{1/4}$-LDHs nanosheets, the current densities at 300 mV were enhanced by 2.6-, 3.4-, and 4.5-folds, respectively, compared with their bulky un-exfoliated phase as shown in Figure 27c.

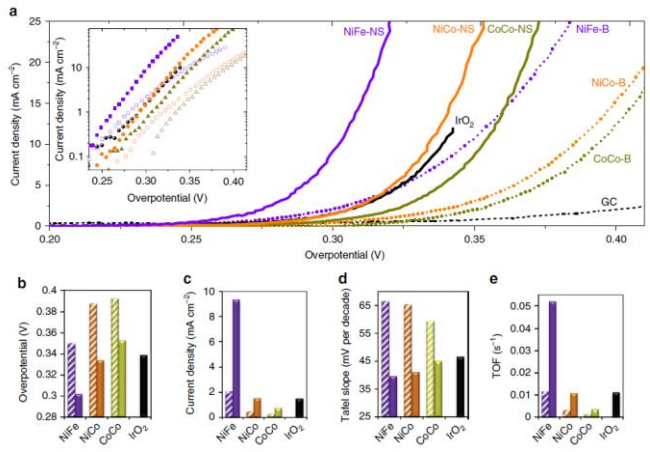

Figure 27. Electrochemical behavior of LDHs materials and IrO_2 nanoparticles. (a) Polarization curves. Inset shows the Tafel plots. Scan rate was 5 mVs^{-1}. The loading was about 0.07 mg/cm^2 for LDHs materials and 0.21 mg/cm^2 for IrO_2 nanoparticles. The electrolyte was 1 M KOH. (b) Overpotential required for J = 10 mA/cm^2. (c) Current densities at η = 300 mV. (d) Tafel slopes. (e) TOF calculated from current at η = 300 mV. $Co_{2/3}/Co_{1/3}$-LDH: yellow-green color; $Ni_{1/3}/Co_{2/3}$-LDH: orange color; $Ni_{3/4}/Fe_{1/4}$-LDH: purple color. Dash lines, hollow symbols and patterned columns: bulk LDHs (B); Solid lines, symbols and columns: exfoliated LDH nanosheets (NS); Black lines, symbols and columns: IrO_2 nanoparticles; GC: glassy carbon electrode.[152] Reproduced with permission from reference 152. Copyright 2014 Macmillan Publishers Limited.

Zhao et al.[141] reported the preparation of Ni_n/Ti_k-LDHs nanosheets (n : k molar ratio varies from 0.83:0.2, 0.76:0.08, 0.82:0.09, to 0.84:0.05) using a reverse micro-emulsion method, which can be used as an efficient photocatalyst for oxygen evolution from water using visible light. The prepared Ni_n/Ti_k-LDHs nanosheets demonstrated extraordinarily high photocatalytic activity (2148 μmol/(g·h) for oxygen evolution from water as shown in Figure 28A. The photocatalytic test was performed by monitoring the time dependent oxygen generation under visible light of λ> 400 nm and $AgNO_3$ was used as a sacrificial reagent. The Ni_n/Ti_k-LDHs nanosheets with a Ni:Ti ratio of 4:1 showed the highest photocatalytic production activity and it remained a high photocatalytic activity over three consecutive cycles (Figure 28B).

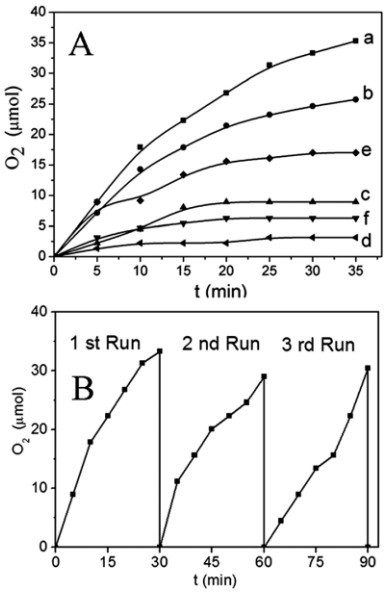

Figure 28. (A) O_2 evolution from aqueous solution using 10^{-2} M $AgNO_3$ as the sacrificial acceptor under visible-light: (a) $Ni_{0.83}/Ti_{0.2}$-LDH, (b) $Ni_{0.76}/Ti_{0.08}$-LDH, (c) $Ni_{0.82}/Ti_{0.09}$-LDH, (d) $Ni_{0.84}/Ti_{0.05}$-LDH, (e) Zn_2/Cr-LDH,[153] (f) WO_3. (B) Catalyst cycling for the photocatalytic generation of oxygen in water in the presence of $Ni_{0.83}/Ti_{0.2}$-LDH.[141] Reproduced with permission from reference 141. Copyright 2014 The Royal Society of Chemistry.

Long et al.[154] reported that a strong coupled hybrid of Fe/Ni_3-LDHs nanosheets and graphene oxide (GO) was an excellent electrocatalyst for oxygen evolution reaction (OER) (Figure 29). The as prepared hybrid exhibited an efficient OER electrocatalytic activity with overpotential as low as 0.21 V and Tafel slope around 40 mV/dec. Moreover, after the reduction of Fe/Ni_3-LDH/GO to Fe/Ni_3-LDH/rGO (reduced graphene oxide), the overpotential of OER was further decreased to 0.195 V and the turnover frequency (TOF) reached 0.98/s at an overpotential of 0.3 V.

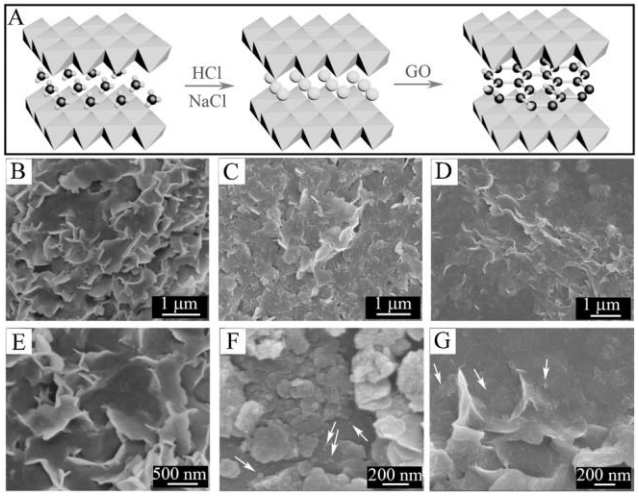

Figure 29. Synthesis and SEM images of Fe/Ni_3-LDH with different anions. (A) Fabrication process of Fe/Ni_3-GO-LDH: Fe/Ni_3-CO_3^{2-}-LDH were dispersed in a HCl and NaCl mixed solution and transformed into Fe/Ni_3-Cl^--LDH, which was further transformed into Fe/Ni_3-GO-LDH hybrid by the anion exchange process. (B)-(G) SEM images of the as prepared Fe/Ni_3-CO_3^{2-}-LDH (B), (E), Fe/Ni_3-Cl^--LDH (C), (F), and Fe/Ni_3-GO-LDH (D), (G) at different magnifications (arrows point at small nanosheets).[154] Reproduced with permission from reference 154. Copyright 2014 John Wiley & Sons, Inc.

More recently, Ma et al.[155] studied the OER activity of a $Ni_{2/3}/Fe_{1/3}$-LDH and graphene superlattice composite. $Ni_{2/3}/Fe_{1/3}$-LDH was synthesized and exfoliated in formamide where its dispersion was mixed with graphene nanosheets based on a calculated hypothetical area matching model to prepare the superlattice composite (Figure 30).

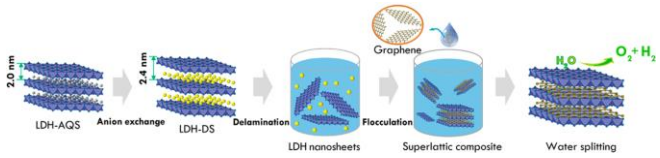

Figure 30. Procedures of hetero-assembling $Ni_{2/3}/Fe_{1/3}$-LDH nanosheets and graphene for water splitting.[155] Reproduced with permission from reference 155. Copyright 2015 The American Chemistry Society.

The prepared $Ni_{2/3}/Fe_{1/3}$-LDH/GO and $Ni_{2/3}/Fe_{1/3}$-LDH/rGO composite, as well as $Ni_{2/3}/Fe_{1/3}$-LDH nanosheets were tested as a catalyst for OER reactions (Figure 31). $Ni_{2/3}/Fe_{1/3}$-LDH/GO and $Ni_{2/3}/Fe_{1/3}$-LDH/rGO exhibited excellent OER efficiency with a low overpotential of 0.23 and 0.21 V, respectively. The authors also found that the prepared composites were active for hydrogen evolution reactions.[155]

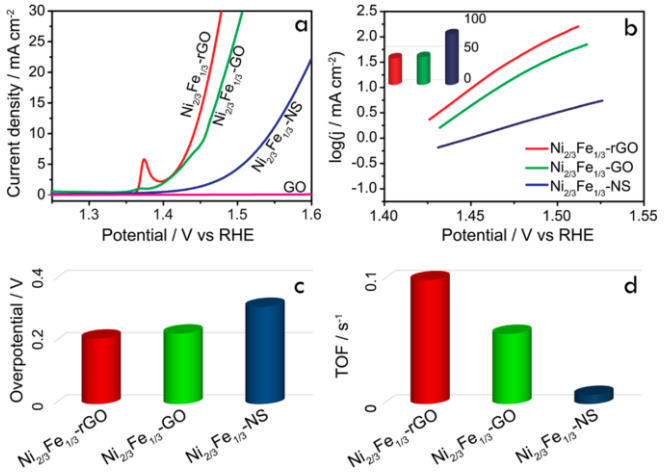

Figure 31. (a) IR-corrected polarization curves of $Ni_{2/3}/Fe_{1/3}$-rGO, $Ni_{2/3}/Fe_{1/3}$-GO, $Ni_{2/3}/Fe_{1/3}$-NS, and GO in 1 M KOH solution; (b) Tafel plots (inset: histogram of corresponding Tafel slopes); (c) overpotential required at 10 mA/cm^2; and (d) TOF at overpotential (0.3 V) of $Ni_{2/3}/Fe_{1/3}$-rGO, $Ni_{2/3}/Fe_{1/3}$-GO, and $Ni_{2/3}/Fe_{1/3}$-NS.[155] Reproduced with permission from reference 155. Copyright 2015 The American Chemistry Society.

3.2 Supercapacitors

Because of its wide range of selection of metal cations, LDHs as a metal oxide precursor or a source of pseudo-capacitive species has attracted increasing attention in supercapacitor research in the past few years.[129, 134, 156-182] For example, Ni_3/Mn-LDH nanosheets were mixed with GO, leading to the instantaneous precipitation of a LDH/GO mixture. After calcination under an inert atmosphere at 450 °C, the hybrid decomposed into Ni_6MnO_8 nanoparticles deposited on larger reconstituted graphene sheets.[183] This resultant hybrid exhibited an electrical conductivity similar to graphite. A maximum capacity value of 1030 mA·h/g was achieved during the first discharge, and capacity values higher than 400 mA·h/g were maintained after 10 cycles. The methodology used in the report was claimed to allow the preparation of a large variety of graphene-metal oxide hybrid materials starting from various LDHs, which possesses the properties from both constituents.

Ma et al.[184] reported a superlattice lamellar hybrid supercapacitor constituted of hetero-stacked LDH nanosheets (positively charged) and GO nanosheets (negatively charged)/or rGO. These hybrids led to a high capacity up to ca. 650 F/g, 6 times higher than the one using pure graphene nanosheets. Electrostatic hetero-assembly experiments were carried out by dropwise addition of anionic GO or rGO nanosheets into the cationic LDH nanosheets dispersion under constant stirring. The precipitates were collected by centrifugation, and then repeatedly dispersed in ethanol and centrifuged. Figure 32 shows the XRD patterns and TEM images of the prepared GO/LDHs and rGO/LDHs hybrids, which confirmed the successful hetero-assembly of LDHs with GO/rGO.

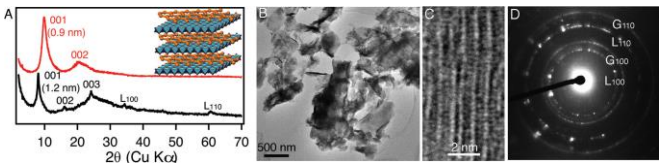

Figure 32. (A) XRD patterns of LDH nanosheets flocculated with GO (black trace) and rGO (red trace) nanosheets, respectively. Indices 00l are basal series of superlattice lamellar composites whereas L_{100} and L_{110} are in-plane diffraction peaks from LDH nanosheets. Inset: schematic illustration of the sandwiched LDH nanosheets and graphene. (B) TEM image of the lamellar nanocomposites. (C) High-resolution TEM image showing lamellar lattice fringes with different contrast appearing at alternating sequence. (D) Electron diffraction indexed to be in-plane diffraction rings of LDHs (L_{100} and L_{110}) and graphene (G_{100} and G_{110}), respectively.[184] Reproduced with permission from reference 184. Copyright 2014 John Wiley & Sons, Inc.

Zhao et al.[185] reported a hierarchical Ni_3/Mn-LDH/carbon nanotube (CNT) hybrid with a superb energy density for flexible supercapacitors. Incorporation of pseudo-capacitive species with carbon-based materials has been extensively studied to realize efficient supercapacitor devices because pseudo-capacitive metal hydroxide/oxide hybrids can provide multiple oxidation states for reversible Faradaic reactions.[186-188] Well-defined 3D structures are extensively studied especially the core-branched structures, where pathways of both electrolyte and electron are built to facilitate efficient energy storage at high rates. Therefore, constructing CNT core (electron pathway) and Ni_3/Mn-LDH branch (electrolyte pathway) was of great importance. Figure 33 shows the synthesis process of the hybrid with well-defined structure. Figure 34a shows the typical CV curves in a potential range of 0-0.6 V at various scan rates, in which the Ni_3/Mn-LDH/CNT hybrid showed the optimum electrochemical performance. Figure 34b presents the galvanostatic charge-discharge measurements, in which Ni_3/Mn-LDH/CNT hybrid led to a specific capacitance as high as 2960 F/g (based on the whole sample mass) at a current density of 1.5 A/g, which is 1.8 times higher than that of the $Ni(OH)_2$/CNT hybrid (1668 F/g). The specific capacitance of the samples at different charge-discharge current densities is shown in Figure 34c, in which the Ni_3/Mn-LDH/CNT hybrid yielded a substantially higher specific capacitance than that of the other samples. At a high current density of 30 A/g, 79.5% of the capacitance (from 2960 to 2338 F/g) was still retained for the supercapacitor with Ni_3/Mn-LDH/CNT, superior to most Ni-based/carbon hybrids.[188, 189] Figure 34d shows the cycling life test, in which the specific capacitance was first increased and then decayed slightly of all the Ni_x/Mn-LDHs/CNT hybrids (x = 2, 3, 5, and 7). After 2000 cycles, the Ni_x/Mn-LDHs/CNT hybrid showed a higher stability and structure integrality with 2.8% loss for Ni_2/Mn-LDH/CNT, 0.9% loss for Ni_3/Mn-LDH/CNT, 2.5% loss for Ni_5/Mn-LDH/CNT, and 3.3% loss for Ni_7/Mn-LDH/CNT.

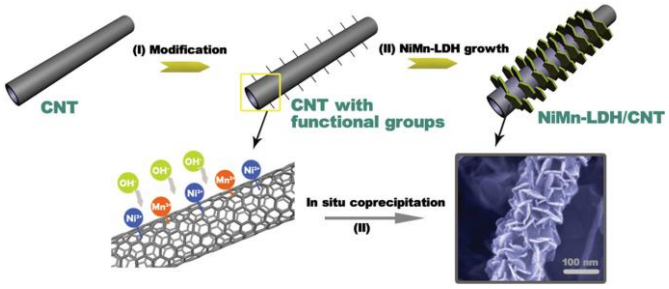

Figure 33. Schematic illustration for the synthesis and morphology of Ni_3/Mn-LDH/CNT. Step (I): surface modification of CNT by functional groups (e.g., $-OH^-$, -CO, $-COO^-$). Step (II): grafting of Ni_3/Mn-LDH nanosheets onto CNT backbone by an in situ growth method.[185] Reproduced with permission from reference 185. Copyright 2014 John Wiley & Sons, Inc.

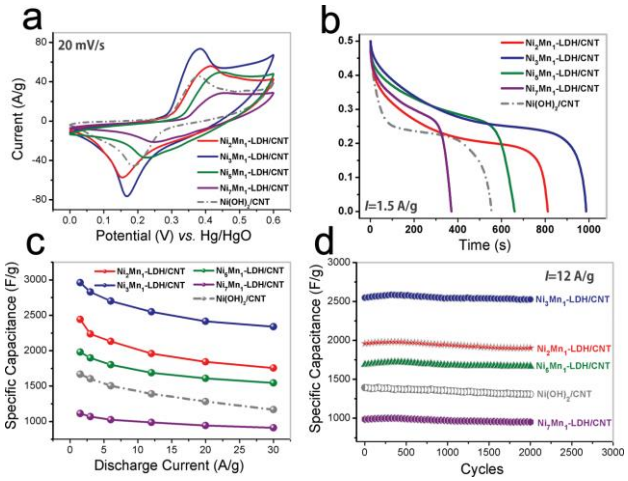

Figure 34. Electrochemical performance of Ni_x/Mn-LDHs/CNT and $Ni(OH)_2$/CNT: (a) CV curves, (b) galvanostatic discharge curves, (c) specific capacitance as a function of current density, and (d) cycle stability.[185] Reproduced with permission from reference 185. Copyright 2014 John Wiley & Sons, Inc.

Yu et al.[190] reported that Co_2/Al-LDH nanosheets electrostatically assembled with modified CNTs exhibited a high specific capacitance of 884 F/g and a high cycle stability over 2000 cycles. Figure 35 illustrates the assembling process, in which the Co_2/Al-CO_3^{2-}-LDH was first anion exchanged to NO_3^--LDH using NH_4NO_3, followed by the exfoliation of the Co_2/Al-NO_3^--LDH by formamide. The obtained LDH nanosheets were subsequently co-assembled with CNTs by shaking CNTs and nanosheets in formamide for a certain period of time.

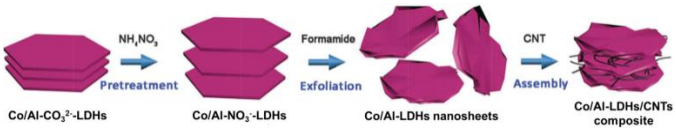

Figure 35. Schematics of each process of assembling the exfoliated Co_2/Al-LDH/CNT hybrid.[190] Reproduced with permission from reference 190. Copyright 2014 The Royal Society of Chemistry.

3.3 Light emitting applications

Recently, the trend of using LDH nanosheets as a host for quantum dots (QDs)/luminescent material has attracted much attention.[191-201] Cho et al.[202] reported the preparation of a highly luminescent and photo-stable composite by incorporating QDs into LDHs matrices with preserved photoluminescence efficiency of the fluorophores. Figure 36A shows the electrostatic assembly process of the QDs-polymer-LDHs nanocomposite by mixing the negatively charged polymer encapsulated CdSe/CdS/ZnS QDs with positively charged Zn_3/Al-LDH nanosheets. QDs-polymer-LDH composite films were prepared by drop casting of the obtained composite dispersion on a substrate. Figure 36B shows the photoluminescence spectra and photographs of the QD-polymer (polymer encapsulated QD) film (I) and the QD-polymer-LDH composite film (II) under UV light. The photoluminescence quantum yield

improvement of QD-polymer-LDH film was attributable to a more uniform distribution of fluorophores thanks to the assistance of LDH nanosheets.

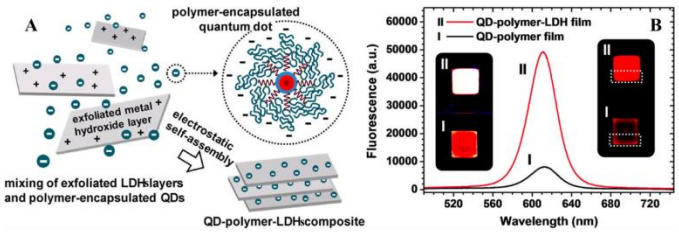

Figure 36. (A) Schematic illustration of the assembly process for the formation of QD-polymer-LDHs composites; (B) Photoluminescence spectra of (I) QD-polymer film and (II) QD-polymer-LDHs composite film. Left inset: photograph of the QD-polymer film and the QD-polymer-LDHs composite film under 60 μW/cm^2 power UV light irradiation. Right inset: photograph of the films under lower power UV light irradiation for color recognition.[202] Reproduced with permission from reference 202. Copyright 2013 The American Chemistry Society.

Tian et al.[203] reported the fabrication of multicolor and white light emitting ultrathin films (UTFs) with 2D architecture utilizing CdTe quantum dots. Stepwise layer-by-layer (LBL) assembly of LDH nanosheets and individual luminescent species was adopted to prepare the hybrid. Figure 37A shows the detailed assembly process of the multi-color UTFs system. The luminescence color of the resulting hybrid UTFs could be easily tuned over the entire visible-light range (Figure 37B), specifically for precisely regulating white emission (Figure 37C), by rational control of the Red/Green/Blue color photo emissive building blocks as well as their sequence.

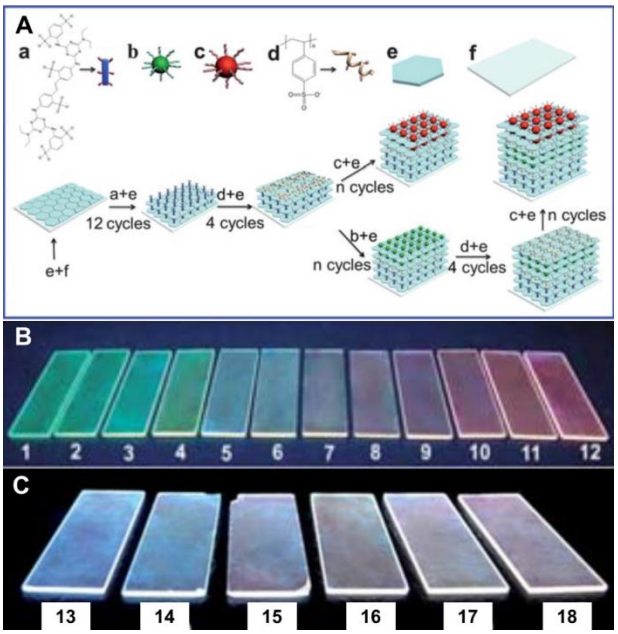

Figure 37. (A) Schematic representation for the LBL fabrication of multilayer luminous UTFs: (a) BTBS (a blue-emitting organic compound, 2,20-(1,2-ethenediyl)bis-[5-[[4-(diethylamino)-6-[(2,5-disulfophenyl)amino]-1,3,5-triazin-2-yl]amino]benzenesulfonic acid] hexasodium salt), (b) QD-530 (green luminescence at 530 nm; particle size: ~2.5 nm), (c) QD-620 (red luminescence at 620 nm; particle size: ~4.0 nm), (d) Poly(sodium 4-styrenesulfonate) (PSS), (e) LDH nanosheets and (f) quartz glass substrate; (B) Photographs of $(BTBS/LDHs)_{12}(QD\text{-}530/LDHs)_{16}(QD\text{-}620/LDHs)_n$ (n = 1 - 12) UTFs under UV light irradiation (365 nm) showing variations of color with n (cycles); (C) Photographs of the $(BTBS/LDHs)_m(QD\text{-}530/LDHs)_n(QD\text{-}620/LDHs)_p$ (m, n, p are the number of cycles of according QDs) UTFs under UV light (365 nm) showing the change in color coordinates in the white-light region.[203] Reproduced with permission from reference 203. Copyright 2013 The Royal Society of Chemistry.

Recently, Cho et al.[204] reported the preparation of photostable composites by assembling near infrared (NIR) emitting PbS based QDs and exfoliated LDH nanosheets for NIR-emitting diodes. The QD-LDHs composite films prepared by drop-casting exhibited NIR photoluminescence over 500% more intensive than the counterpart QD films (without the LDHs matrix) under identical conditions.

3.4 Flame retardant

Well dispersed LDH nanosheets in polymer matrices can greatly improve the flame retardancy of polymers.[205, 206] It is believed that the release of H_2O (from the interlayer water and/or the decomposition of metal hydroxide layers) and gases (such as CO_2 from CO_3^{2-}) during thermal decomposition of LDHs can effectively lower heat release rate. Dispersion is crucial to achieve a high flame retardancy of polymer/LDHs composites, which have been extensively studied.[207] Wang et al.[208] reported a single step self-assembly method to prepare organically modified Co_2/Al-LDH polypropylene (O-Co_2/Al-LDH-PP) composites with enhanced flame retardant properties. The addition of partially exfoliated organo-Co_2/Al-LDH filler into PP at a high level of dispersion led to a significant decrease of the heat release rate (HRR), the total heat release (THR), and the heat release capacity (HRC) of the PP composites, as shown in Figure 38 and Table 2. With an increasing LDHs filler concentration, the peak heat release rate (PHRR) value decreased significantly as shown in Table 2.

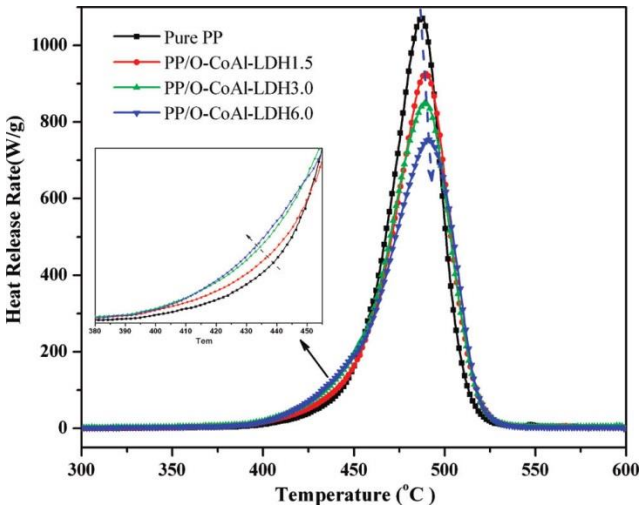

Figure 38. Heat release rate curves for PP and a PP/O-Co_2/Al-LDH*N* nanocomposite at 1 K/s heating rate (PP/O–Co_2/Al–LDH*N*, *N* = 1.5, 3.0 and 6.0 (parts per hundred resin), indicates the concentration of LDH in the composite).[208] Reproduced with permission from reference 208. Copyright 2010 The American Chemistry Society.

Table 2. Summary of microscale combustion colorimetry measurements for PP/O-Co_2/Al-LDH nanocomposites.[208] Reproduced with permission from reference 208. Copyright 2010 The American Chemistry Society.

Sample	PHRR (W/g)	THR [kJ/g]	T_{-max} [°C]	HRC [J/g K]
PP	1071	38.8	487	1055
PP/O–Co_2/Al–LDH1.5	926	37.7	489	900
PP/O–Co_2/Al–LDH3.0	848	37.4	489	830
PP/O–Co_2/Al–LDH6.0	754	32.2	491	798

The flame retardancy and thermal degradation of the epoxy nanocomposites containing graphene nanosheets (GNS) and LDHs were studied by Liu et al.[209] The additional GNS/LDHs interface created by the simultaneous addition of both materials into the epoxy resin (ER) increased the interaction of LDHs and GNS in the melt, inducing inhibition of flammable drips of ER and limiting the flame propagation due to the increased interaction of LDHs and GNS in the melt. As shown in Figure 39, after the limiting oxygen index (LOI) test, the neat ER sample exhibited melt dripping, while the dripping phenomenon was not observed in the ER/GNS, ER/LDHs, ER/GNS/LDHs nanocomposites.

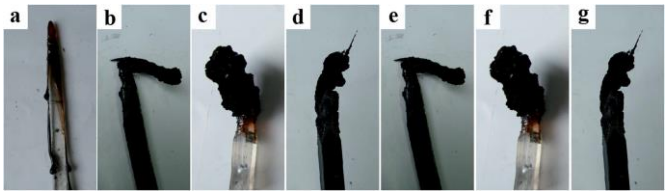

Figure 39. Patterns of the samples after LOI tests: (a) ER, (b) ER/GNS1, (c) ER/LDHs1, (d) ER/GNS0.5/LDHs0.5, (e) ER/GNS5, (f) ER/LDHs5, and (g) ER/GNS2.5/LDHs2.5. (The samples are identified as mass ratio of ER/GNS*x* = 100/*x*, ER/LDHs*y* = 100/*y*, and ER/GNS*x*/LDHs*y* = 100/*x*/*y*).[209] Reproduced with permission from reference 209. Copyright 2014 The Royal Society of Chemistry.

Kuila et al.[210] reported a rubber/LDHs nanocomposite made of ethylene vinyl acetate (EVA) (60 wt% in the rubber) and DS^--modified LDHs (DS^--LDHs) via a solution intercalation method where the intercalation of the polymer in LDHs at various loadings were studied. The result showed that at 1 wt% and 3-8 wt% DS^--LDHs loadings, fully exfoliated LDHs and partially exfoliated LDHs formed, respectively. The premium mechanical properties of the nanocomposites were found at 3 wt% of DS^--LDHs loading. Compared with the neat EVA (2.6 MPa), the tensile strength of the rubber composite containing 3 wt% DS^--LDHs increased to 5.1 MPa, representing a 96% improvement. Thermal stability of the EVA/DS^--LDHs nanocomposites was improved by 12-15 °C with respect to the neat EVA. The LOI test confirmed the improved flame retardant properties. More examples are referred to Gao et al.[211] who reviewed the recent examples of polymer/LDHs composites for flame retardancy.

4. Conclusion and outlook

In this review, we endeavor to summarize existing methods to prepare single-layer LDH nanosheets. Top-down exfoliation and bottom-up direct synthesis methods represent two typical categories of approaches to obtain LDH nanosheets. We divided the top-down methods into two main categories: tailor the interlayer environment for exfoliation and exfoliation driven by mechanical force. The former one focused on creating a hydrogen-bonding rich environment, enabling the introduction of a large amount of solvent to separate LDHs layers. The latter one proposed a mechanism from a swollen phase to an exfoliated phase where the swollen LDHs in formamide has to undergo extensive mechanical agitation to be exfoliated. The bottom-up approaches adopt either a chemical environment or a mechanical environment to grow LDH nanosheets directly. Overall, at present the bottom-up methods appear to be advantageous favoring large scale production of dispersible LDH nanosheets. However, such routes have their own disadvantages, including suffering from either the utilization of toxic dispersants or from the difficulties in recovering LDH nanosheets from their chemical environment.

Over the past decade, new applications of LDH nanosheets involving catalyzing water splitting reaction, supporting QDs, and formulating flame retardants and supercapacitors have surfaced. We briefly overview the promising results of LDHs catalysts in producing oxygen through electrical as well as photocatalytic routes, LDHs supports for QDs in light emitting units, LDHs flame retardant substitutes for halogens in polymer composites. Many new and significant achievements have been made in the applications of LDH nanosheets. However, tough challenges are still to be addressed. In general, direct use of stable LDH nanosheets dispersion in an exfoliated form remains an issue due to unavoidable aggregation during separation from the dispersants. Utilization of dispersed LDH nanosheets in catalyzing water splitting reactions is rather exciting, but the exact catalytic mechanism is to be completely revealed so that researchers can design and synthesize the most suitable LDHs nanosheet catalysts. Fabricating LDHs/polymer flame retardant composites requires surface modification of hydrophilic LDHs into hydrophobic one to maximize its dispersion in polymer matrices. Moreover, to achieve a high level of flame retardancy, synergistic effect of LDHs and traditional flame retardant materials such as organophosphorus compounds should be further explored and investigated. Researches in LDH nanosheets in electronics such as supercapacitors are very active, significant advancement in such fields is anticipated in the near future. LDH nanosheets, thanks to their versatility in component metal cations and their sheet structure with a high surface area, will remain highly attractive to researchers in chemistry, materials, and engineering. We anticipate applications utilizing highly dispersed LDH nanosheets will continue to expand in the coming years.

Abbreviations

LDHs	=	Layered double hydroxides
SOS	=	Sodium octyl sulfate
SDS	=	Sodium dodecyl sulfate
SOBS	=	Sodium 4-octylbenzenesulfonate
SDBS	=	Sodium dodecylbenzenesulfonate
DBS	=	Dodecylbenzenesulfonate
HEMA	=	2-Hydroxyethyl methacrylate
PS	=	Polystyrene

LLDPE	=	Linear low density polyethylene
PE-g-MA anhydride	=	polyethylene-grafted-maleic
AFM	=	Atomic force microscopy
HMT	=	Hexamethylenetetramine
AUA	=	11-aminoundecanoic acid
Nd:YAG garnet	=	Neodymium:yttrium-aluminum-
GO	=	Graphene oxide
OER	=	Oxygen evolution reaction
TOF	=	Trunover frequency
CNT	=	Carbon nanotube
QDs	=	Quantum dots
UTFs	=	Ultrathin films
LBL	=	Layer-by-layer
BTBS	=	2,20-(1,2-ethenediyl)bis-[5-[[4-(diethylamino)-6-[(2,5-disulfophenyl)amino]-1,3,5-triazin-2-yl]amino]benzenesulfonic acid] hexasodium salt
QD-530	=	Green luminescence at 530 nm; particle size: ~2.5 nm
QD-620	=	Red luminescence at 620 nm; particle size: ~4 nm
PSS	=	Poly(sodium 4-styrenesulfonate)
NIR	=	Near infrared
O-Co_2Al-LDH-PP	=	Organically modified Co_2Al-LDH polypropylene composite
HRR	=	Heat release rate
THR	=	Total heat release
HRC	=	Heat release capacity
PHRR	=	Peak heat release rate
PP	=	Polypropylene
PP/O-Co_2Al-LDH*N*	=	The O-Co_2Al-LDH-PP contains *N* parts of O-Co_2Al-LDH (unite: parts per hundred resin)
GNS	=	Graphene nanosheets
ER	=	Epoxy resin
LOI	=	Limiting oxygen index
EVA	=	Ethylene vinyl acetate

Acknowledgements

L. Sun acknowledges the support from the National Science Foundation (CMMI-1562907) and the Faculty Large Grant from the University of Connecticut. D. O'Hare and Q. Wang thanks SCG Chemicals Co., Ltd for support.

References

1. E. L. P. Crepaldi, P. C.; Valim, J. B., *J. Mater. Chem.*, 2000, **10**, 1337-1343.
2. K. Itaya, H. C. Chang and I. Uchida, *Inorg. Chem.*, 1987, **26**, 624-626.
3. J. W. Gilman, *Applied Clay Science*, 1999, **15**, 31-49.
4. K. A. Carrado and L. Xu, *Chem. of Mater.*, 1998, **10**, 1440-1445.
5. X. Fu and S. Qutubuddin, *Polymer*, 2001, **42**, 807-813.
6. A. Akelah and A. Moet, *Journal of Materials Science*, 1996, **31**, 3589-3596.
7. A. Okada and A. Usuki, *Materials Science and Engineering: C*, 1995, **3**, 109-115.
8. T. Kuila, H. Acharya, S. K. Srivastava and A. K. Bhowmick, *Polymer Composites*, 2009, **30**, 497-502.
9. E. Kafunkova, K. Lang, P. Kubat, M. Klementova, J. Mosinger, M. Slouf, A.-L. Troutier-Thuilliez, F. Leroux, V. Verney and C. Taviot-Gueho, *J. Mater. Chem.*, 2010, **20**, 9423-9432.
10. S. Lv, W. Zhou, H. Miao and W. Shi, *Progress in Organic Coatings*, 2009, **65**, 450-456.
11. Y. Gao, Y. Zhang, G. R. Williams, D. O'Hare and Q. Wang, *Scientific reports*, 2016, **6,** 35502-35514.
12. H. Huang, J. Xu, K. Wei, Y. J. Xu, C. K. K. Choi, M. Zhu and L. Bian, *Macromolecular bioscience*, 2016, **16**, 1019-1026.
13. E. N. Kalali, X. Wang and D.-Y. Wang, *Journal of Materials Chemistry A*, 2016, **4**, 2147-2157.
14. G. Abellan, J. L. Jorda, P. Atienzar, M. Varela, M. Jaafar, J. Gomez-Herrero, F. Zamora, A. Ribera, H. Garcia and E. Coronado, *Chemical Science*, 2015, **6**, 1949-1958.
15. A. C. Perreira, S. Pearson, D. Kostadinova, F. Leroux, F. D'Agosto, M. Lansalot, E. Bourgeat-Lami and V. Prevot, *Polymer Chemistry*, 2017, **8**, 1233-1243.
16. F. Millange, R. I. Walton, L. Lei and D. O'Hare, *Chem. Mater.*, 2000, **12**, 1990-1994.
17. P. K. Dutta and M. Puri, *The Journal of Physical Chemistry*, 1989, **93**, 376-381.
18. L. Kullberg and A. Clearfield, *The Journal of Physical Chemistry*, 1981, **85**, 1585-1589.
19. T.-Y. Tsai, C.-K. Wen, H.-J. Chuang, M.-J. Lin and U. Ray, *Polymer Composites*, 2009, **30**, 1552-1561.
20. M. Zubair, M. Daud, G. McKay, F. Shehzad and M. A. Al-Harthi, *Applied Clay Science*, 2017, **143**, 279-292.
21. Q. He, S. Yin and T. Sato, *J. Phys. Chem. Solids*, 2004, **65**, 395-402.
22. D. S. Robins and P. K. Dutta, *Langmuir*, 1996, **12**, 402-408.
23. L. A. Vermeulen and M. E. Thompson, *Chem. Mater.*, 1994, **6**, 77-81.
24. H. Nakajima, S. Ishino, H. Masuda, T. Shimosaka, T. Nakagama, T. Hobo and K. Uchiyama, *Chem. Lett.*, 2005, **34**, 358-359.
25. H. Tagaya, S. Ogata, S. Nakano, J.-I. Kadokawa, M. Karasu and K. Chiba, *Journal of Inclusion Phenomena and Macrocyclic Chemistry*, 1998, **31**, 231-241.
26. P. Atienzar, M. de Victoria-Rodriguez, O. Juanes, J. C. Rodriguez-Ubis, E. Brunet and H. Garcia, *Energy & Environmental Science*, 2011, **4**, 4718-4726.
27. J. L. Colon, C. Y. Yang, A. Clearfield and C. R. Martin, *The Journal of Physical Chemistry*, 1990, **94**, 874-882.
28. J. Liu, F. Wang and X. Xu, *Cata. Lett.*, 2008, **120**, 106-110.
29. F. Wang, J. Liu and X. Xu, *Chem. Commun.*, 2008, **0**, 2040-2042.
30. B. M. Choudary, M. Lakshmi Kantam, C. R. Venkat Reddy, K. Koteswara Rao and F. Figueras, *J. Mol. Catal. A: Chem.,* 1999, **146**, 279-284.
31. P. S. Kumbhar, *Chem. Commun.*, 1998, **10**, 1091-1092.
32. B. M. Choudary, S. Madhi, N. S. Chowdari, M. L. Kantam and B. Sreedhar, *Journal of the American Chemical Society*, 2002, **124**, 14127-14136.
33. S. Velu, N. Shah, T. M. Jyothi and S. Sivasanker, *Microporous and Mesoporous Materials*, 1999, **33**, 61-75.
34. W. Kagunya, Z. Hassan and W. Jones, *Inorg. Chem.*, 1996, **35**, 5970-5974.
35. G. Centi and S. Perathoner, *Microporous and Mesoporous Materials*, 2008, **107**, 3-15.
36. F. E. Osterloh, *Chem. Mater.*, 2007, **20**, 35-54.
37. P. Lu, S. Liang, L. Qiu, Y. Gao and Q. Wang, *Journal of Membrane Science*, 2016, **504**, 196-205.
38. L. Mohapatra and K. Parida, *Journal of Materials Chemistry A*, 2016, **4**, 10744-10766.
39. Y. Tokudome, T. Morimoto, N. Tarutani, P. D. Vaz, C. D. Nunes, V. Prevot, G. B. Stenning and M. Takahashi, *ACS nano*, 2016, **10**, 5550-5559.
40. C. Zhang, M. Shao, L. Zhou, Z. Li, K. Xiao and M. Wei, *ACS Applied Materials & Interfaces*, 2016, **8**, 33697-33703.
41. C. Wang, B. Ma, S. Xu, D. Li, S. He, Y. Zhao, J. Han, M. Wei, D. G. Evans and X. Duan, *Nano Energy*, 2017, **32**, 463-469.
42. F. Cavani, F. TrifirÃ² and A. Vaccari, *Catalysis Today*, 1991, **11**, 173-301.
43. G. Fan, F. Li, D. G. Evans and X. Duan, *Chem. Soc. Rev.*, 2014, **43**, 7040-7066.

44. Q. Wang and D. O'Hare, *Chem. Rev.*, 2012, **112**, 4124-4155.
45. J. Yu, B. R. Martin, A. Clearfield, Z. Luo and L. Sun, *Nanoscale*, 2015, **7**, 9448-9451.
46. M. Daud, M. S. Kamal, F. Shehzad and M. A. Al-Harthi, *Carbon*, 2016, **104**, 241-252.
47. J. Qu, Q. Zhang, X. Li, X. He and S. Song, *Applied Clay Science*, 2016, **119**, 185-192.
48. S. Omwoma, W. Chen, R. Tsunashima and Y. F. Song, *Coordination Chemistry Reviews*, 2014, **s 258–259**, 58-71.
49. V. Rives, *Materials Chemistry and Physics*, 2002, **75**, 19-25.
50. S. Carlino, *Solid State Ionics*, 1997, **98**, 73-84.
51. K.-H. Goh, T.-T. Lim and Z. Dong, *Water Research*, 2008, **42**, 1343-1368.
52. J. Zhang, H. Hu, Z. Li and X. W. Lou, *Angew. Chem. Int. Ed.*, 2016, **55**, 3982-3986.
53. R. Sasai and M. Morita, *Sensors and Actuators B: Chemical*, 2017, **238**, 702-705.
54. X. Long, Z. Wang, S. Xiao, Y. An and S. Yang, *Mater. Today*, 2016, **19**, 213-226.
55. L. Zhou, M. Shao, C. Zhang, J. Zhao, S. He, D. Rao, M. Wei, D. G. Evans and X. Duan, *Adv. Mater.*, 2017, **29**, 1604080-1604087.
56. S. Huang, H. Peng, W. W. Tjiu, Z. Yang, H. Zhu, T. Tang and T. Liu, *The Journal of Physical Chemistry B*, 2010, **114**, 16766-16772.
57. R. Ma, Z. Liu, L. Li, N. Iyi and T. Sasaki, *J. Mater. Chem.*, 2006, **16**, 3809-3813.
58. L. Li, R. Ma, Y. Ebina, N. Iyi and T. Sasaki, *Chem. Mater.*, 2005, **17**, 4386-4391.
59. K. Okamoto, K. Tamura, M. Takahashi and A. Yamagishi, *Colloids and Surfaces A: Physicochemical and Engineering Aspects*, 2000, **169**, 241-249.
60. H. Yin and Z. Tang, *Chem. Soc. Rev.*, 2016, **45**, 4873-4891.
61. J. He, M. Wei, B. Li, Y. Kang, D. Evans and X. Duan, *Layered double hydroxides*, 2006, 89-119.
62. S. P. Newman and W. Jones, *New J. Chem.*, 1998, **22**, 105-115.
63. Z. P. Xu and G. Q. Lu, *Chem. Mater.*, 2005, **17**, 1055-1062.
64. Y. Zhao, F. Li, R. Zhang, D. G. Evans and X. Duan, *Chem. Mater.*, 2002, **14**, 4286-4291.
65. T. Hibino and H. Ohya, *Applied Clay Science*, 2009, **45**, 123-132.
66. H. Kang, M. Leoni, H. He, G. Huang and X. Yang, *Eur. J. Inorg. Chem.*, 2012, **2012**, 3859-3865.
67. U. Costantino, F. Marmottini, M. Nocchetti and R. Vivani, *Eur. J. Inorg. Chem.*, 1998, **1998**, 1439-1446.
68. N. Iyi, T. Matsumoto, Y. Kaneko and K. Kitamura, *Chem. Lett.*, 2004, **33**, 1122-1123.
69. L. Sun, W. J. Boo, R. L. Browning, H.-J. Sue and A. Clearfield, *Chem. of Mater.*, 2005, **17**, 5606-5609.
70. L. Sun, J. Y. O'Reilly, D. Kong, J. Y. Su, W. J. Boo, H. J. Sue and A. Clearfield, *Journal of Colloid and Interface Science*, 2009, **333**, 503-509.
71. M. Meyn, K. Beneke and G. Lagaly, *Inorganic Chemistry*, 1990, **29**, 5201-5207.
72. W. Hou, L. Kang, R. Sun and Z.-H. Liu, *Colloids and Surfaces A: Physicochemical and Engineering Aspects*, 2008, **312**, 92-98.
73. J. M. Hidalgo, Jim, S. nez, C. n, sar, M. Mora, J. Ruiz and Rafael, *Journal of Nanoscience and Nanotechnology*, 2010, **10**, 6562-6566.
74. M. Adachi-Pagano, C. Forano and J.-P. Besse, *Chem. Commun.*, 2000, **0**, 91-92.
75. M. Singh, M. I. Ogden, G. M. Parkinson, C. E. Buckley and J. Connolly, *Journal of Materials Chemistry*, 2004, **14**, 871-874.
76. B. R. Venugopal, C. Shivakumara and M. Rajamathi, *J. Colloid Interface Sci.*, 2006, **294**, 234-239.
77. M. Ì. a. JobbÃ¡gy and A. E. Regazzoni, *J. Colloid Interface Sci.*, 2004, **275**, 345-348.
78. V. V. Naik, T. N. Ramesh and S. Vasudevan, *The Journal of Physical Chemistry Letters*, 2011, **2**, 1193-1198.
79. V. V. Naik and S. Vasudevan, *Langmuir*, 2011, **27**, 13276-13283.
80. S. O'Leary, D. O'Hare and G. Seeley, *Chemical Communications*, 2002, **14**, 1506-1507.
81. L. Qiu, W. Chen and B. Qu, *Polymer Degradation and Stability*, 2005, **87**, 433-440.
82. L. Du and B. Qu, *J. Mater. Chem.*, 2006, **16**, 1549-1554.
83. W. Chen and B. Qu, *Chem. Mater.*, 2003, **15**, 3208-3213.
84. W. Chen, L. Feng and B. Qu, *Chem. Mater.*, 2004, **16**, 368-370.
85. T. Hibino and W. Jones, *J. Mater. Chem.*, 2001, **11**, 1321-1323.
86. T. Hibino, *Chem. Mater.*, 2004, **16**, 5482-5488.
87. F. Wypych, G. A. Bubniak, M. Halma and S. Nakagaki, *J. Colloid Interface Sci.*, 2003, **264**, 203-207.
88. Y. H. Bao-guang Li, Zu-Yao, *Chin. J. Chem. Phys.* , 2006, **19**, 253-258.
89. U. Ugur, *J. Solid State Chem.*, 2007, **180**, 2525-2533.
90. N. Iyi, T. Matsumoto, Y. Kaneko and K. Kitamura, *Chem. Mater.*, 2004, **16**, 2926-2932.
91. K. Okamoto, T. Sasaki, T. Fujita and N. Iyi, *J. Mater. Chem.*, 2006, **16**, 1608-1616.
92. Z. Liu, R. Ma, M. Osada, N. Iyi, Y. Ebina, K. Takada and T. Sasaki, *Journal of the American Chemical Society*, 2006, **128**, 4872-4880.
93. Y. Omomo, T. Sasaki, Wang and M. Watanabe, *Journal of the American Chemical Society*, 2003, **125**, 3568-3575.
94. T. Sasaki and M. Watanabe, *Journal of the American Chemical Society*, 1998, **120**, 4682-4689.
95. T. Sasaki, M. Watanabe, H. Hashizume, H. Yamada and H. Nakazawa, *Journal of the American Chemical Society*, 1996, **118**, 8329-8335.
96. Z. Liu, R. Ma, Y. Ebina, N. Iyi, K. Takada and T. Sasaki, *Langmuir*, 2006, **23**, 861-867.
97. G. Abellan, E. Coronado, C. Marti-Gastaldo, E. Pinilla-Cienfuegos and A. Ribera, *J. Mater. Chem.*, 2010, **20**, 7451-7455.
98. Q. Wu, A. Olafsen, O. B. Vistad, J. Roots and P. Norby, *J. Mater. Chem.*, 2005, **15**, 4695-4700.
99. R. Ma, Z. Liu, K. Takada, N. Iyi, Y. Bando and T. Sasaki, *Journal of the American Chemical Society*, 2007, **129**, 5257-5263.
100. R. Ma, K. Takada, K. Fukuda, N. Iyi, Y. Bando and T. Sasaki, *Angew. Chem. Int. Ed.*, 2008, **47**, 86-89.
101. J. Liang, R. Ma, N. Iyi, Y. Ebina, K. Takada and T. Sasaki, *Chem. Mater.*, 2009, **22**, 371-378.
102. H. Kang, G. Huang, S. Ma, Y. Bai, H. Ma, Y. Li and X. Yang, *The Journal of Physical Chemistry C*, 2009, **113**, 9157-9163.
103. L. Chen, B. Sun, X. Wang, F. Qiao and S. Ai, *Journal of Materials Chemistry B*, 2013, **1**, 2268-2274.
104. J. Wang, L. Huang, Y. Gao, R. Yang, Z. Zhang, Z. Guo and Q. Wang, *Chem. Commun.*, 2014, **50**, 10130-10132.
105. E. Gardner, K. M. Huntoon and T. J. Pinnavaia, *Adv. Mater.*, 2001, **13**, 1263-1266.
106. T. Hibino and M. Kobayashi, *J. Mater. Chem.*, 2005, **15**, 653-656.
107. C. Jaubertie, M. J. Holgado, M. S. San Román and V. Rives, *Chem. Mater.*, 2006, **18**, 3114-3121.
108. M. S. San Román, M. J. Holgado, C. Jaubertie and V. Rives, *Solid State Sciences*, 2008, **10**, 1333-1341.
109. K. Okudaira, Y. Kameshima, T. Isobe, A. Nakajima and K. Okada, *Journal of the Japan Society of Colour Material*, 2010, **84**, 2-6.
110. G. V. Manohara, D. A. Kunz, P. V. Kamath, W. Milius and J. Breu, *Langmuir*, 2010, **26**, 15586-15591.
111. C. A. Antonyraj, P. Koilraj and S. Kannan, *Chem. Commun.*, 2010, **46**, 1902-1904.
112. Y. Wei, F. Li and L. Liu, *RSC Advances*, 2014, **4**, 18044-18051.
113. G. Hu, N. Wang, D. O'Hare and J. Davis, *Chem. Commun.*, **3**, 2006, 287-289.
114. F. Bellezza, A. Cipiciani, U. Costantino, M. Nocchetti and T. Posati, *Eur. J. Inorg. Chem.*, 2009, **2009**, 2603-2611.

115. Y. Yan, Q. Liu, J. Wang, J. Wei, Z. Gao, T. Mann, Z. Li, Y. He, M. Zhang and L. Liu, *J. Colloid Interface Sci.*, 2012, **371**, 15-19.
116. J. Yu, J. Liu, A. Clearfield, J. E. Sims, M. T. Speiegle, S. L. Suib and L. Sun, *Inorg. Chem.*, 2016, **55**, 12036-12041.
117. B. M. Hunter, J. D. Blakemore, M. Deimund, H. B. Gray, J. R. Winkler and A. M. Müller, *J. Am. Chem. Soc.*, 2014, **136**, 13118-13121.
118. T.-B. Hur, T. X. Phuoc and M. K. Chyu, *J. Appl. Phys.*, 2010, **108**, 114312-114317.
119. X. Pang, M. Sun, X. Ma and W. Hou, *J. Solid State Chem.*, 2014, **210**, 111-115.
120. J. Li, W. Xu, R. Li, J. Luo, D. Zhou, S. Li, P. Cheng and D. Yuan, *Journal of Materials Science*, 2016, **51**, 9287-9295.
121. K. Yan, T. Lafleur, J. Chai and C. Jarvis, *Electrochem. Commun.*, 2016, **62**, 24-28.
122. H. Liu, Y. Wang, X. Lu, Y. Hu, G. Zhu, R. Chen, L. Ma, H. Zhu, Z. Tie, J. Liu and Z. Jin, *Nano Energy*, 2017, **35**, 350-357.
123. J. Ping, Y. Wang, Q. Lu, B. Chen, J. Chen, Y. Huang, Q. Ma, C. Tan, J. Yang, X. Cao, Z. Wang, J. Wu, Y. Ying and H. Zhang, *Adv. Mater.*, 2016, **28**, 7640-7645.
124. C. Zhang, J. Zhao, L. Zhou, Z. Li, M. Shao and M. Wei, *Journal of Materials Chemistry A*, 2016, **4**, 11516-11523.
125. N. Han, F. Zhao and Y. Li, *Journal of Materials Chemistry A*, 2015, **3**, 16348-16353.
126. H. Liang, F. Meng, M. Cabán-Acevedo, L. Li, A. Forticaux, L. Xiu, Z. Wang and S. Jin, *Nano Lett.*, 2015, **15**, 1421-1427.
127. J. Jiang, A. Zhang, L. Li and L. Ai, *J. Power Sources*, 2015, **278**, 445-451.
128. C. Qiao, Y. Zhang, Y. Zhu, C. Cao, X. Bao and J. Xu, *Journal of Materials Chemistry A*, 2015, **3**, 6878-6883.
129. Y. Hou, M. R. Lohe, J. Zhang, S. Liu, X. Zhuang and X. Feng, *Energy & Environmental Science*, 2016, **9**, 478-483.
130. J. Ping, Y. Wang, Q. Lu, B. Chen, J. Chen, Y. Huang, Q. Ma, C. Tan, J. Yang and X. Cao, *Adv. Mater.*, 2016, **28**, 7640-7645.
131. W. Ma, R. Ma, J. Wu, P. Sun, X. Liu, K. Zhou and T. Sasaki, *Nanoscale*, 2016, **8**, 10425-10432.
132. Y. Vlamidis, E. Scavetta, M. Gazzano and D. Tonelli, *Electrochim. Acta*, 2016, **188**, 653-660.
133. D. Zhao, K. Jiang, Y. Pi and X. Huang, *ChemCatChem*, 2017, **9**, 84-88.
134. F. Gu, X. Cheng, S. Wang, X. Wang and P. S. Lee, *Small*, 2015, **11**, 2044-2050.
135. J. Bao, X. Zhang, B. Fan, J. Zhang, M. Zhou, W. Yang, X. Hu, H. Wang, B. Pan and Y. Xie, *Angew. Chem.*, 2015, **127**, 7507-7512.
136. C. Qiao, Y. Zhang, Y. Zhu, C. Cao, X. Bao and J. Xu, *Journal of Materials Chemistry A*, 2015, **3**, 6878-6883.
137. X. Long, S. Xiao, Z. Wang, X. Zheng and S. Yang, *Chem. Commun.*, 2015, **51**, 1120-1123.
138. J. A. Carrasco, J. Romero, M. Varela, F. Hauke, G. Abellán, A. Hirsch and E. Coronado, *Inorganic Chemistry Frontiers*, 2016, **3**, 478-487.
139. B. Ni and X. Wang, *Chemical Science*, 2015, **6**, 3572-3576.
140. F. Song and X. Hu, *J. Am. Chem. Soc.*, 2014, **136**, 16481-16484.
141. Y. Zhao, B. Li, Q. Wang, W. Gao, C. J. Wang, M. Wei, D. G. Evans, X. Duan and D. O'Hare, *Chemical Science*, 2014, **5**, 951-958.
142. N. Han, F. Zhao and Y. Li, *Journal of Materials Chemistry A*, 2015, **3**, 16348-16353.
143. J. L. Gunjakar, I. Y. Kim, J. M. Lee, N.-S. Lee and S.-J. Hwang, *Energy & Environmental Science*, 2013, **6**, 1008-1017.
144. J. Wu, Z. Ren, S. Du, L. Kong, B. Liu, W. Xi, J. Zhu and H. Fu, *Nano Res*, 2016, **9**, 713-725.
145. Y. Jia, L. Zhang, G. Gao, H. Chen, B. Wang, J. Zhou, M. T. Soo, M. Hong, X. Yan, G. Qian, J. Zou, A. Du and X. Yao, *Adv. Mater.*, 2017, **29**, 1700017-1700024.
146. P. F. Liu, S. Yang, B. Zhang and H. G. Yang, *ACS Applied Materials & Interfaces*, 2016, **8**, 34474-34481.
147. X. Jia, Y. Zhao, G. Chen, L. Shang, R. Shi, X. Kang, G. I. N. Waterhouse, L.-Z. Wu, C.-H. Tung and T. Zhang, *Advanced Energy Materials*, 2016, **6**, 1502585-1502590.
148. Z. Wang, S. Zeng, W. Liu, X. Wang, Q. Li, Z. Zhao and F. Geng, *ACS Applied Materials & Interfaces*, 2017, **9**, 1488-1495.
149. Y. Wang, Y. Zhang, Z. Liu, C. Xie, S. Feng, D. Liu, M. Shao and S. Wang, *Angew. Chem.*, 2017, **56**, 5867-5872.
150. B. M. Hunter, H. B. Gray and A. M. Müller, *Chem. Rev.*, 2016, **116**, 14120-14136.
151. B. M. Hunter, W. Hieringer, J. R. Winkler, H. B. Gray and A. M. Muller, *Energy & Environmental Science*, 2016, **9**, 1734-1743.
152. F. Song and X. Hu, *Nature Communications*, 2014, **5**, 4477-4485.
153. C. G. Silva, Y. Bouizi, V. Fornés and H. García, *J. Am. Chem. Soc.*, 2009, **131**, 13833-13839.
154. X. Long, J. Li, S. Xiao, K. Yan, Z. Wang, H. Chen and S. Yang, *Angew. Chem. Int. Ed.*, 2014, **53**, 7584-7588.
155. W. Ma, R. Ma, C. Wang, J. Liang, X. Liu, K. Zhou and T. Sasaki, *ACS Nano*, 2015, **9**, 1977-1984.
156. K. Ma, J. P. Cheng, F. Liu and X. Zhang, *J. Alloys Compd.*, 2016, **679**, 277-284.
157. Y. Gu, Z. Lu, Z. Chang, J. Liu, X. Lei, Y. Li and X. Sun, *Journal of Materials Chemistry A*, 2013, **1**, 10655-10661.
158. S. C. Sekhar, G. Nagaraju and J. S. Yu, *Nano Energy*, 2017, **36**, 58-67.
159. D. Zha, H. Sun, Y. Fu, X. Ouyang and X. Wang, *Electrochim. Acta*, 2017, **236**, 18-27.
160. F. Lai, Y.-E. Miao, L. Zuo, H. Lu, Y. Huang and T. Liu, *Small*, 2016, **12**, 3235-3244.
161. G. Nagaraju, G. S. R. Raju, Y. H. Ko and J. S. Yu, *Nanoscale*, 2016, **8**, 812-825.
162. Y. Zhao, Q. Wang, T. Bian, H. Yu, H. Fan, C. Zhou, L.-Z. Wu, C.-H. Tung, D. O'Hare and T. Zhang, *Nanoscale*, 2015, **7**, 7168-7173.
163. Z. Huang, S. Wang, J. Wang, Y. Yu, J. Wen and R. Li, *Electrochim. Acta*, 2015, **152**, 117-125.
164. F. He, Z. Hu, K. Liu, S. Zhang, H. Liu and S. Sang, *J. Power Sources*, 2014, **267**, 188-196.
165. H. Chen, L. Hu, M. Chen, Y. Yan and L. Wu, *Adv. Funct. Mater.*, 2014, **24**, 934-942.
166. F. Lai, Y. E. Miao, L. Zuo, H. Lu, Y. Huang and T. Liu, *Small*, 2016, **12**, 3235-3244.
167. J. Wu, W.-W. Liu, Y.-X. Wu, T.-C. Wei, D. Geng, J. Mei, H. Liu, W.-M. Lau and L.-M. Liu, *Electrochim. Acta*, 2016, **203**, 21-29.
168. X. L. Guo, X. Y. Liu, X. D. Hao, S. J. Zhu, F. Dong, Z. Q. Wen and Y. X. Zhang, *Electrochim. Acta*, 2016, **194**, 179-186.
169. R. Zhang, H. An, Z. Li, M. Shao, J. Han and M. Wei, *Chem. Eng. J.*, 2016, **289**, 85-92.
170. M. Li, J. Cheng, J. Wang, F. Liu and X. Zhang, *Electrochim. Acta*, 2016, **206**, 108-115.
171. F. Lai, Y. E. Miao, L. Zuo, H. Lu, Y. Huang and T. Liu, *Small*, 2016, **12**, 3199-3199.
172. X. Li, J. Zai, Y. Liu, X. He, S. Xiang, Z. Ma and X. Qian, *J. Power Sources*, 2016, **325**, 675-681.
173. X. Wang, Y. Zheng, J. Yuan, J. Shen, J. Hu, A.-J. Wang, L. Wu and L. Niu, *Electrochim. Acta*, 2017, **224**, 628-635.
174. C. Wang, X. Zhang, X. Sun and Y. Ma, *Electrochim. Acta*, 2016, **191**, 329-336.
175. F. Lai, Y. Huang, Y.-E. Miao and T. Liu, *Electrochim. Acta*, 2015, **174**, 456-463.
176. K. Ma, J. Cheng, J. Zhang, M. Li, F. Liu and X. Zhang, *Electrochim. Acta*, 2016, **198**, 231-240.
177. G. Nagaraju, G. S. R. Raju, Y. H. Ko and J. S. Yu, *Nanoscale*, 2016, **8**, 812-825.
178. C. Wang, X. Zhang, Z. Xu, X. Sun and Y. Ma, *ACS applied materials & interfaces*, 2015, **7**, 19601-19610.
179. Y. Lu, B. Jiang, L. Fang, F. Ling, F. Wu, B. Hu, F. Meng, K. Niu, F. Lin and H. Zheng, *J. Alloys Compd.*, 2017, **714**, 63-70.

180. L. Zhang, H. Yao, Z. Li, P. Sun, F. Liu, C. Dong, J. Wang, Z. Li, M. Wu, C. Zhang and B. Zhao, *J. Alloys Compd.*, 2017, **711**, 31-41.
181. T. Wang, S. Zhang, X. Yan, M. Lyu, L. Wang, J. Bell and H. Wang, *ACS Applied Materials & Interfaces*, 2017, **9**, 15510-15524.
182. X. Wang, X. Li, X. Du, X. Ma, X. Hao, C. Xue, H. Zhu and S. Li, *Electroanalysis*, 2017, **29**, 1-9.
183. M. Latorre-Sanchez, P. Atienzar, G. Abellán, M. Puche, V. Fornés, A. Ribera and H. García, *Carbon*, 2012, **50**, 518-525.
184. R. Ma, X. Liu, J. Liang, Y. Bando and T. Sasaki, *Adv. Mater.*, 2014, **26**, 4173-4178.
185. J. Zhao, J. Chen, S. Xu, M. Shao, Q. Zhang, F. Wei, J. Ma, M. Wei, D. G. Evans and X. Duan, *Adv. Funct. Mater.*, 2014, **24**, 2938-2946.
186. Y. Cheng, S. Lu, H. Zhang, C. V. Varanasi and J. Liu, *Nano Letters*, 2012, **12**, 4206-4211.
187. C. Yuan, L. Yang, L. Hou, J. Li, Y. Sun, X. Zhang, L. Shen, X. Lu, S. Xiong and X. W. Lou, *Adv. Funct. Mater.*, 2012, **22**, 2560-2566.
188. Z. Tang, C.-h. Tang and H. Gong, *Adv. Funct. Mater.*, 2012, **22**, 1272-1278.
189. P. Lin, Q. She, B. Hong, X. Liu, Y. Shi, Z. Shi, M. Zheng and Q. Dong, *Journal of the Electrochemical Society*, 2010, **157**, A818-A823.
190. L. Yu, N. Shi, Q. Liu, J. Wang, B. Yang, B. Wang, H. Yan, Y. Sun and X. Jing, *Physical Chemistry Chemical Physics*, 2014, **16**, 17936-17942.
191. Y. Yu, J. Shi, X. Zhao, Z. Yuan, C. Lu and J. Lu, *Analyst*, 2016, **141**, 3305-3312.
192. M. Liu, T. Wang, H. Ma, Y. Fu, K. Hu and C. Guan, *Scientific Reports*, 2014, **4**, 7147-7155.
193. Y. Qin, J. Lu, S. Li, Z. Li and S. Zheng, *The Journal of Physical Chemistry C*, 2014, **118**, 20538-20544.
194. Y. Qin, J. Lu, S. Li, Z. Li and S. Zheng, *The Journal of Physical Chemistry C*, 2014, **118**, 20538-20544.
195. R. Gao and D. Yan, *Chemical Science*, 2017, **8**, 590-599.
196. R. Tian, S. Zhang, M. Li, Y. Zhou, B. Lu, D. Yan, M. Wei, D. G. Evans and X. Duan, *Adv. Funct. Mater.*, 2015, **25**, 5006-5015.
197. Z. Li, R. Liang, S. Xu, W. Liu, D. Yan, M. Wei, D. G. Evans and X. Duan, *Nano Research*, 2016, **9**, 3828-3838.
198. X. Wu, J.-G. Li, Q. Zhu, W. Liu, J. Li, X. Li, X. Sun and Y. Sakka, *Journal of Materials Chemistry C*, 2015, **3**, 3428-3437.
199. Q. Zhu, Z. Xu, J.-G. Li, X. Li, Y. Qi and X. Sun, *Nanoscale research letters*, 2015, **10**, 132-144.
200. K.-H. Lee, B.-I. Lee, J.-H. You and S.-H. Byeon, *Chem. Commun.*, 2010, **46**, 1461-1463.
201. M. Liu, T. Wang, H. Ma, Y. Fu, K. Hu and C. Guan, *Scientific reports*, 2014, **4**, 7147-7155.
202. S. Cho, J. Kwag, S. Jeong, Y. Baek and S. Kim, *Chem. Mater.*, 2013, **25**, 1071-1077.
203. R. Tian, R. Liang, D. Yan, W. Shi, X. Yu, M. Wei, L. S. Li, D. G. Evans and X. Duan, *Journal of Materials Chemistry C*, 2013, **1**, 5654-5660.
204. S. Cho, S. C. Hong and S. Kim, *Journal of Materials Chemistry C*, 2014, **2**, 450-457.
205. W. Wang, H. Pan, Y. Shi, Y. Pan, W. Yang, K. Liew, L. Song and Y. Hu, *Composites Part A: Applied Science and Manufacturing*, 2016, **80**, 259-269.
206. H. Pan, W. Wang, Q. Shen, Y. Pan, L. Song, Y. Hu and Y. Lu, *RSC Advances*, 2016, **6**, 111950-111958.
207. Z. Matusinovic and C. A. Wilkie, *J. Mater. Chem.*, 2012, **22**, 18701-18704.
208. D.-Y. Wang, A. Das, F. R. Costa, A. Leuteritz, Y.-Z. Wang, U. Wagenknecht and G. Heinrich, *Langmuir*, 2010, **26**, 14162-14169.
209. S. Liu, H. Yan, Z. Fang, Z. Guo and H. Wang, *RSC Advances*, 2014, **4**, 18652-18659.
210. T. Kuila, S. K. Srivastava and A. K. Bhowmick, *J. Appl. Polym. Sci.*, 2009, **111**, 635-641.
211. Y. Gao, J. Wu, Q. Wang, C. A. Wilkie and D. O'Hare, *Journal of Materials Chemistry A*, 2014, **2**, 10996-11016.